République Algérienne Démocratique et Populaire
Ministère de l'Enseignement Supérieur et de la Recherche Scientifique

Université Hadj Lakhdar Batna
Faculté de Technologie
Département d'Électronique

Mémoire

Présenté pour l'obtention du diplôme de
MAGISTER en Électronique

OPTION

Traitement du Signal

Par

Asma BOUNOUARA

Thème

QRS Detection In ECG Signals

Soutenu devant le jury composé de :

Dr. Moussa BENYOUCEF	Professeur.	Université de Batna	Président
Dr. Nabil BENOUDJIT	Professeur.	Université de Batna	Rapporteur
Dr. Noureddine GHOGGALI	Maitre de conférences.	Université de Batna	Co-rapporteur
Dr. Abdelhamid BENAKCHA	Professeur.	Université de Biskra	Examinateur
Dr. Redha BENZID	Professeur.	Université de Batna	Examinateur

Décembre 2015

People.s Democratic Republic of Algeria
Ministry of Higher Education and Scientific Research
University of Batna 02
Faculty of Technology
Department of Electronics

A Dissertation Presented
in partial fulfilment of the requirement
for the degree of ***Magister*** In Electronics
OPTION: Signal processing

By

Asma BOUNOUARA

QRS Detection In ECG Signals

Examination committee

Dr. Moussa BENYOUCEF	Professor.	University of Batna	President
Dr. Nabil BENOUDJIT	Professor.	University of Batna	supervisor
Dr. Noureddine GHOGGALI	Maître de conferences.	University of Batna	Co-supervisor
Dr. Abdelhamid BENAKCHA	Professor.	University of Biskra	reviewer
Dr. Redha BENZID	Professor.	University of Batna	reviewer

December 2015

Table of Contents

Acknowledgment

Firstly, I thank **Allah**, the Most High, for the opportunity He gave me to study, to research and to write this dissertation. **Thank Allah,** my outmost thanks, for giving me the ability, the strength, attitude and motivation through this research and to complete this work.
I wish to express my special gratitude to my supervisors **Professor Nabil BENOUDJIT** and **Dr. Noureddine GHOGGALI** for accepting supervise me as a student at the Department of Electronics. I am sincerely grateful for your guidance, wisdom, and specially your endless patients in dealing with me throughout all these years. It is difficult to overstate my gratitude to you, with your enthusiasm, your inspiration, and your great efforts make this approach easier. Many thanks to you for assisting me throughout my thesis-writing period; you provided encouragement, sound advice, and lots of good ideas. Thank you for believing me and for giving me good advice, support and freedom along the way.

I would like to thank **Professor Moussa BENYOUSSEF** from University of Batna for being president of the examination committee. I would like to thank my oral thesis committee members, **Professor Redha BENZID** from University of Batna, **Dr. Abdelhamid BENAKCHA** from University of Biskra for accepting the examination of this thesis.

I would like to thank all my friends, colleagues and the staff at the Department of Electronics, University of Batna for their help along the realisation of this work.

My deep gratitude is due, ***to my parents*** for their devotion, sacrifices, continuous guidance, encouragement, support, and prayers for my whole life. Thanks are due, ***to my husband, my brothers and my sister*** for their cooperation and help. I also want to ***thank all my immediate and extended family members*** for all their love and support.

Abstract

The Electrocardiogram ECG is a fundamental part of cardiovascular assessment. It is an essential tool for investigating cardiac arrhythmias and is also useful in diagnosing cardiac disorders such as myocardial infarction. The importance of the electrical activity of the heart has attracted attention of many scientists in the domain of diagnostic pathology in the myocardium due to the fact that theirs electrical activity can be the source of a wealth of valuable information on the state structure and function of the cardiovascular system. Because the QRS complex is the major feature in ECG signal, we applied Pan and Tompkins algorithm to detect the location of the R-peak in the ECG signal and later we try to improve as an improvement to this, we belive that the well choose of certain free parameter described in the original paper will results in an increase of the detection capability.

Keywords : ECG, R-peaks, Pan and Tompkins.

Résumé

L'électrocardiogramme ECG est un élément fondamental de l'évaluation cardiovasculaire système. C'est un outil essentiel pour examiner les arythmies cardiaques et également utile dans le diagnostic des troubles cardiaques comme l'infarctus du myocarde. L'importance de l'activité électrique du cœur a attiré l'attention de nombreux scientifiques dans le domaine de la pathologie de diagnostic dans le myocarde due au fait que leur activité électrique peut être la source de plusieurs informations précieuses sur la structure de l'état et le fonctionnement du système cardiovasculaire. Parce que le complexe QRS est la caractéristique majeure du signal ECG, nous avons appliqué Pan et Tompkins algorithme pour détecter l'emplacement de R-pic dans le signal ECG. Comme amélioreation pour ce dernier, nous croyant que le choix judicieux de certain parametr decrit dans le papier original aurra un impact positif en term de detection .

Mots-clés: ECG, R-pic, Pan et Tompkins.

الملخص

التخطيط الكهربائية للقلب ECG هو جزء أساسي من تقييم عمل القلب والأوعية الدموية. وهو أداة أساسية للتحقيق في عدم انتظام ضربات القلب ومفيد أيضا في تشخيص اضطرابات القلب مثل احتشاء عضلة القلب. النشاط الكهربائي للقلب جذب اهتمام العديد من العلماء في مجال التشخيص المرضي في عضلة القلب و يرجع ذلك إلى حقيقة أن النشاط الكهربائي يمكن أن يكون مصدرا للعديد من المعلومات القيمة عن حالة وظيفة نظام القلب والأوعية الدموية. ويعد مجمع QRS خاصية رئيسية في إشارة ECG، طبقنا خوارزمية Pan و Tompkins للكشف عن مكان وجود R-ذروة في إشارة ECG. كما تحاول تحسين القدرة على الكشف عن هذه الخوارزمية، حاولنا إثبات نتائج الكشف عن مجمع QRS في هذه الخوارزمية قمنا بغيير بعض المعايير الحرة المكتوبة في المقال الاصلي مما أدى إلى زيادة في القدرة على كشف مجمع QRS.

الكلمات- المفتاحية : Pan و Tompkins ، R-ذروة ، ECG

LIST OF FIGURES

General Introduction

Chapter I

Chapter II

Chapter III

Chapter IV

LIST OF TABLES

Chapter IV

Introduction

Electrocardiography

The heart is one of the most important and critical organ in the human body, thus the need to develop a method for automatic monitoring its functionality is extremely important. Electrocardiography is considered to be one of the most powerful diagnostic tools in medicine that is periodically used for the evaluation of the functionality of the heart. The electrocardiogram (ECG) is the traditional method for non-invasive interpretation of the electrical activity of the heart in real-time. The electrical cardiac signals are recorded by mean of external sensors, by connecting electrodes to the surface of the skin of the patient's thorax. The electrical currents stimulate the cardiac muscle and cause the contractions and relaxations of the heart [1]. The electrical signals sensed by the sensors are sent to the ECG device, which records them as feature waves. Different waves reflect the activity of different areas of the heart which generate the respective flowing electrical current. Figure 1 shows a schematic representation of normal ECG and its diverse waves.

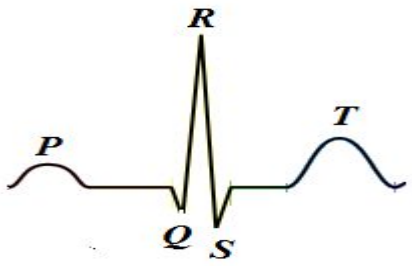

Figure 1 Normal ECG with the waves that is consisted noted.

Characteristics of normal electrocardiogram

A normal ECG consists of P wave, a QRS complex, and T wave. The P wave is generated by electric currents produced by the depolarization of the atria before their contraction, while the QRS complex is caused by electric currents produced by the depolarization of the ventricles prior to their contraction, during the extending of the depolarization in the ventricular myocardium [2]. The QRS complex commonly consist of three different waves, the Q, R and S waves it's worth noting that both the P wave, and the waves that form the QRS complex, are depolarization waves. The electric currents produced during recovery of the ventricles from the state of depolarization are the causative factor of the T wave. This process takes place in the ventricular myocardium 0.25s to 0.35s after the depolarization. The T wave has the peculiarity to be the wave of repolarization.

Why is the ECG important?

The ECG has been established as the most common and easiest way for accurate and rapid diagnosis and management of numerous cardiovascular incidents. A significant number of patients treated in the emergency room (ER) and in the intensive care unit (ICU), present with cardiovascular complaints. In those cases, the needs of early, accurate diagnosis as well as rapid, appropriate therapy reinforce the importance of electrocardiography. Some examples of incidents that are ideally managed with an ECG are chest pain (presenting ST segment elevation), acute myocardial infarction, acute coronary syndrome, arrhythmias, and even suspected pulmonary embolism [2].

Principal methods for ECG analysis

Nowadays digital electrocardiography is a well established practice, after many years of significant improvement. Many algorithms have been proposed over years to tackle the issue of the QRS detection in the ECG signal and classification. Because the QRS complex is the most significant waveform the ECG detection is the first step in every automated algorithm for ECG analysis owing to their characteristic shape, the QRS complexes serve as reference point for the automatic heart rate detection analysis and feature extraction. The QRS complex detection has been a research topic for more than many years. Numerous new approaches have been proposed in the literature, in order to find the best automatic QRS detection method [3].

Artifacts in the ECG signal

Unfortunately the acquired of the ECG signal does not only include the useful components derived from the electrical functionality of the heart, but very often contain artifacts that can interfere the signal and result in a degradation/loss of the quality of the signal. Sometimes, these artifacts might even present with morphology which are similar to the ECG [4]. The most commonly found noises in the ECG are:

1. Power line interference.
2. Baseline drift.
3. Muscle contraction (EMG).
4. Movement artifacts.

The influence of artifacts in the ECG signal significantly makes its analysis difficult if not impossible. This occurs because there is a high overlap between the artifacts and the signal, scarce work has been done on artifacts detection and removal and thus the literature found on this subject

is rather limited. In general those methods can only minimize the influence of some artifacts, but in the majority of the cases they are enable the totally remove the artifacts.

Purpose and motivation

The purpose of this thesis was to analyze the ECG signal and more specifically, to apply the method described by the Pan and Tompkins algorithm for the detection of the QRS complexes. To avoid erroneous results, at first the QRS identification should goes to detection and removal phase from the ECG signal, so that the QRS detection would be more robust.

The ECG data used for this work was found in the PhysioNet library (http://physionet.org). This physiological database provided by the collaboration between Massachusetts Institute of Technology and Boston's Beth Israel Hospital (MIT/BIH). The MIT/BIH arrhythmia database contains 48 half hour of two channel ambulatory ECG recording, obtained from 47 subjects studied by the BIH arrhythmia laboratory .The subjects were 25 men aged between 32 and 89 years and 22 women aged between 23 and 89 years. This database contains lots of labelled artifacts by human experts, which interfere with the normal and abnormal ECG signals.

The adopted method for successful artifacts detection and removal and then QRS complex detection, was achieved by linear filtering, non-linear transformation and decision rule algorithm. The first step is to use a digital band pass filter to eliminate all the high frequency and to reduces false detections caused by the various artifacts present in ECG signals, in the next step is to differentiated the filtered signal to get information about the slope of the QRS complex, the non-linear transformation is the squared step, it used to amplify the output of derivation stage and finally computed integral of each moving window to quantify QRS and non-QRS. And an adaptive thresholds is done for both band pass and integrated signal to improve the of the QRS detection.

The outline of our work plan includes four chapters; the first chapter will be devoted to the basic notion of the main element of the cardiovascular system, the heart. The second chapter is assigned to acquisition of the electrocardiogram and the most component of ECG signal. Chapter three discusses the adapted solution of the QRS complex detection algorithm (Pan and Tompkins algorithm). We finished this modest work by reporting the results of the filtering phase performed on the ECG signals of the standard database MIT/BIH and the results of the QRS complex detection by the implemented algorithm. We finished this work by a conclusion and a suggesting of some ideas in the future work.

Chapter I

Basic notions of cardiology

Introduction

The human heart located in the mediastinum, is the central element of the cardiovascular system. It is protected by the bony structures of the sternum anteriorly, the spinal column posteriorly and rib cage, is a muscle that works continuously, it can be considered as a pump that pumps blood throughout the body by means of a coordinated contraction. The contraction is generated by an electrical signal activation, which is spread by a wave of bioelectricity that propagates in a coordinated manner throughout the heart.

Under normal conditions, the sinoatrial node initiates an electrical impulse that propagates through the atria to the atrioventricular node, where a delay permits ventricular filling before the electrical impulse proceeds through the specialized His-Purkinje conduction system that spreads the electrical signal throughout the ventricles. This electrical impulse propagates through the heart and elevates the voltage at each cell, producing an action potential, during which a surge in intracellular calcium initiates the mechanical contraction. The normal rhythm is altered when one or more spiral waves of electrical activity appear. These waves are life-threatening because they behave as high-frequency sources and underlie complex cardiac electrical dynamics such as tachycardia and fibrillation [5]. We present in the next section the general functioning of the cardiovascular system and the basic notions of cardiology.

I Anatomy and physiology of the heart

I.1 Location of the Heart

In the cardiovascular system the human heart is the most important element, which is named a muscle infarction. It is the organ that supplies blood and oxygen to all parts of the body. It is located in the chest between the lungs behind, the sternum and above the diaphragm. It is surrounded by the pericardium. Its size is about that of a fist, and its weight is about 250-300 g. Its center is located about 1.5 cm to the left of the midsagittal plane. Located above the heart are the great vessels: the superior and inferior vena cava, the pulmonary artery and vein, as well as the aorta. The aortic arch lies behind the heart.

The esophagus and the spine lie further behind the heart. An overall view is given in Figure 1.1 [6].

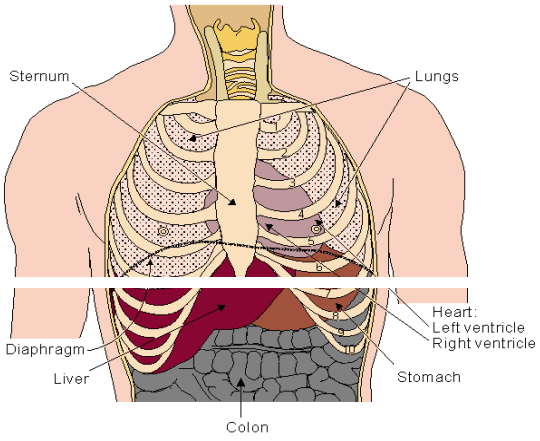

Figure 1.1 Location of the heart in the thorax. It is bounded by the diaphragm, lungs, esophagus, descending aorta, and sternum.

I.2 Anatomy of the Heart

I.2.1 The heart's chambers

The walls of the heart are composed of cardiac muscle, called myocardium. It also has striations similar to skeletal muscle. It consists of four chambers that work in pairs: the right atrium, the right ventricle, the left atrium, and the left ventricle. The right ventricle is the lower right chamber of the heart. During the normal cardiac cycle, the right ventricle receives deoxygenated blood as the right atrium contracts. During this process the pulmonary valve is closed, allowing the right ventricle to fill. Once both ventricles are full, they contract. As the right ventricle contracts, the tricuspid valve closes and the pulmonary valve opens. The closure of the tricuspid valve prevents blood from returning to the right atrium, and the opening of the pulmonary valve allows the blood to flow into the pulmonary artery toward the lungs for oxygenation of the blood. The right and left ventricles contract simultaneously; however, because the right ventricle is thinner than the left, it produces a lower pressure than the left when contracting. This lower pressure is sufficient to pump the deoxygenated blood the short distance to the lungs. Left ventricle is the lower left chamber of the heart. During the normal cardiac cycle, the left ventricle receives oxygenated blood through the mitral valve from the left atrium as it contracts. At the same time, the aortic valve leading to the aorta is closed, allowing the ventricle to fill with blood. Once both ventricles are full, they contract. As the left ventricle contracts, the mitral valve closes and the aortic valve opens. The closure of the mitral valve prevents

blood from returning to the left atrium, and the opening of the aortic valve allows the blood to flow into the aorta and from there throughout the body. The left and right ventricles contract simultaneously; however, because the left ventricle is thicker than the right, it produces a higher pressure than the right when contracting. This higher pressure is necessary to pump the oxygenated blood throughout the body. Right atrium is the upper right chamber of the heart. During the normal cardiac cycle, the right atrium receives deoxygenated blood from the body (blood from the head and upper body arrives through the superior vena cava, while blood from the legs and lower torso arrives through the inferior vena cava). Once both atria are full, they contract, and the deoxygenated blood from the right atrium flows into the right ventricle through the open tricuspid valve. Left atrium is the upper left chamber of the heart. During the normal cardiac cycle, the left atrium receives oxygenated blood from the lungs through the pulmonary veins. Once both atria are full, they contract, and the oxygenated blood from the left atrium flows into the left ventricle through the open mitral valve [1]. Figure 1.2 shows the heart's chambers.

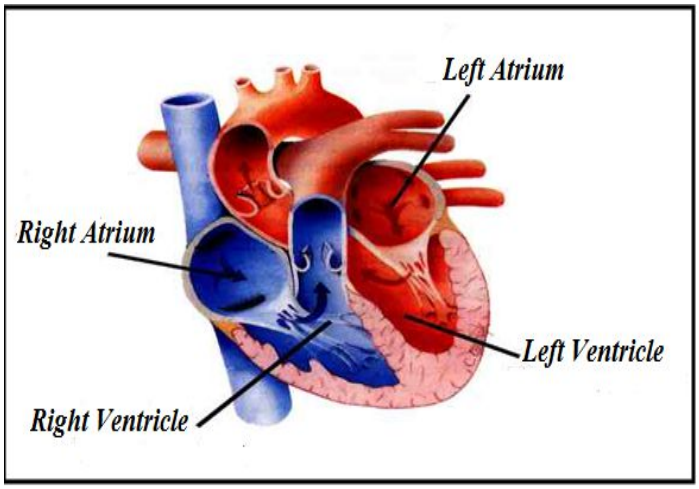

Figure 1.2 the heart's chambers.

I.2.2 The heart's valves

A group of four valves controls the flow of blood within the heart. These valves prevent blood moving in the wrong direction through the heart. The valves are located between each atrium and ventricle and in the two arteries that empty blood from the ventricle [4].

- **Aortic Valve:** also called a semi-lunar valve separates the left ventricle from the aorta. As the ventricles contract, it opens to allow the oxygenated blood collected in the left

ventricle to flow throughout the body. It closes as the ventricles relax, preventing blood from returning to the heart. Valves on the heart's left side need to withstand much higher pressures than those on the right side. Sometimes they can wear out and leak or become thick and stiff.

- **Mitral Valve**: also called Bicuspid separates the left atrium from the left ventricle. It opens to allow the oxygenated blood collected in the left atrium to flow into the left ventricle. It closes as the left ventricle contracts, preventing blood from flowing backwards to the left atrium and thereby forcing it to exit through the aortic valve into the aorta. The mitral valve has tiny cords attached to the walls of the ventricles. This helps support the valve's small flaps or leaflets.
- **Pulmonary Valve**: separates the right ventricle from the pulmonary artery. As the ventricles contract, it opens to allow the deoxygenated blood collected in the right ventricle to flow to the lungs. It closes as the ventricles relax, preventing blood from returning to the heart.
- **Tricuspid Valve**: Located between the right atrium and the right ventricle, the tricuspid valve is the first valve that blood encounters as it enters the heart. When open, it allows the deoxygenated blood collected in the right atrium to flow into the right ventricle. It closes as the right ventricle contracts, preventing blood from flowing backwards to the right atrium, thereby forcing it to exit through the pulmonary valve into the pulmonary artery. Figure 1.3 shows the heart's valves.

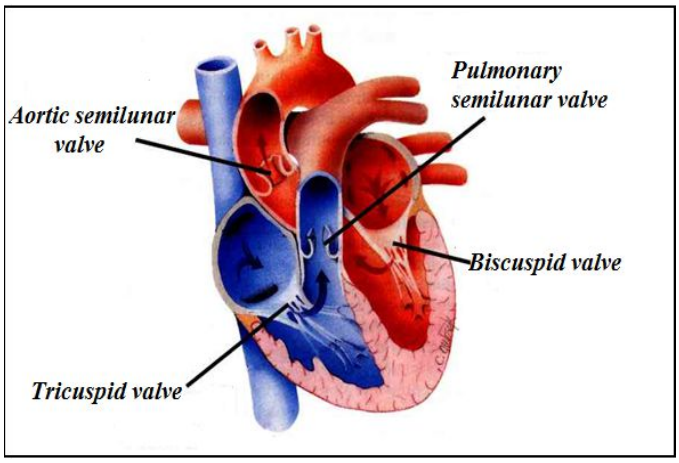

Figure 1.3 The heart's valves.

I.3The blood circulation System

The major vessels of the heart are the large arteries and veins that attach to the atria, ventricles and transport blood to and from the systemic circulatory system and pulmonary

circulation system. Blood is delivered to the right atrium from the systemic circulatory system by two veins. The superior vena cava transport oxygen-depleted blood from the upper extremities, heard and neck. The inferior vena cava transport oxygen-depleted blood from the thorax, abdomen and lower extremities. Blood exits the right ventricles through the pulmonary trunk artery. Approximately two inches superior to the base of the heart, this vessel branches into the left and right pulmonary arteries, which transport blood into the lungs. The left pulmonary veins and right pulmonary veins return oxygen-ated blood from the lungs to the left atrium. Blood passes from the left atrium into the left ventricle and then is pumped into the systemic circulatory system through a large elastic artery called the aorta [4]. An overall view of the blood circulation system is given in Figure 1.4, in which the red circulatory system indicates the flow of oxygenated blood coming from the lungs, flowing into the left atrium of the heart, and pumped out to the body by the left ventricle. The blue circulatory system indicates the flow of blood low in oxygen coming from the body, returning to the right atrium of the heart and pumped out to the lungs by the right ventricle.

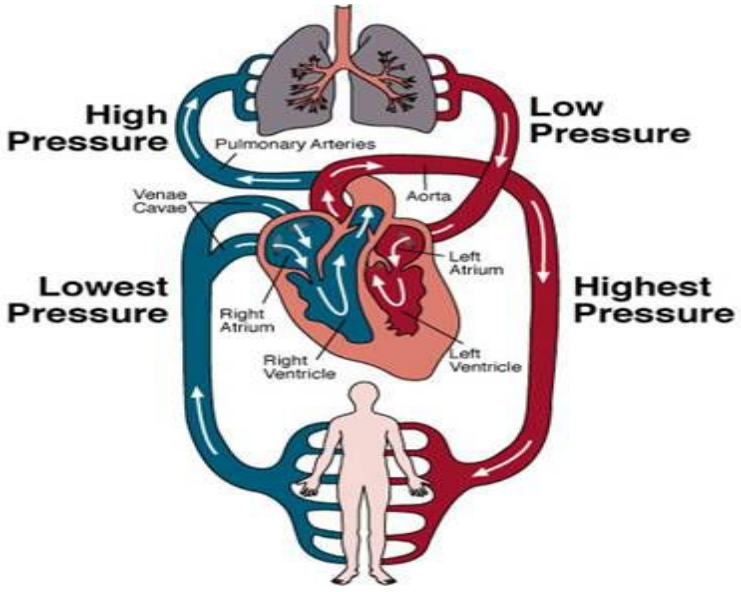

Figure 1.4 The Circulation System.

I.4 The cardiac cycle

The cardiac cycle is a period from the beginning of one heart beat to the beginning of the next one .A single cycle of cardiac activity can be divided into two basic phases **diastole** and **systole** as shown in next Figure [7].

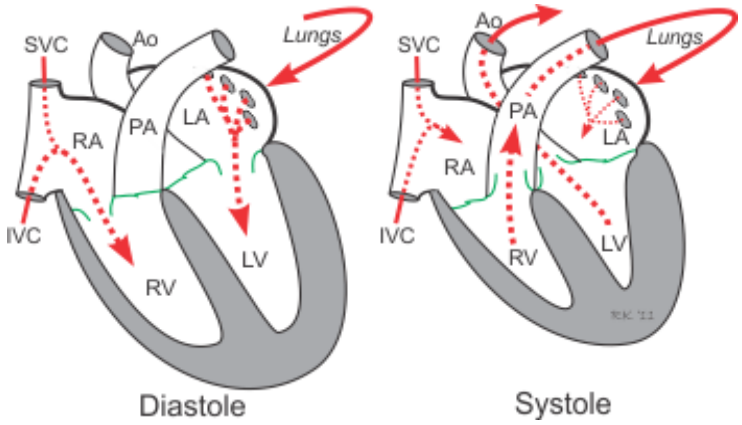

Figure 1.5 The cardiac cycle.

Diastole represents the period of time when the ventricles are relaxed (not contracting).Throughout most of this period, blood is passively flowing from the left atrium (LA) and right atrium (RA) into the left ventricle (LV) and right ventricle (RV), respectively. The blood flows through atrioventricular valves (mitral and tricuspid) that separate the atria from the ventricles. The RA receives venous blood from the body through the superior vena cava (SVC) and inferior vena cava (IVC). The LA receives oxygenated blood from lungs through four pulmonary veins that enter the LA. At the end of diastole, both atria contract, this propels an additional amount of blood into the ventricles.

Systole represents the time during which the left and right ventricles contract and eject blood into the aorta and pulmonary artery, respectively. During systole, the aortic and pulmonic valves open to permit ejection into the aorta and pulmonary artery. The atrioventricular valves are closed during systole, therefore no blood is entering the ventricles; however, blood continues to enter the atria though the vena cavae and pulmonary veins [7].

The duration of the cardiac cycle is inversely proportional to the heart rate. The cardiac cycle duration increases with a decrease in the heart rate and on the other hand it shortens with increasing heart rate. At a normal heart rate of 75 beats per minute, one cardiac cycle lasts 0.8 second. Under resting conditions, systole occupies ⅓ and diastole ⅔ of the cardiac cycle duration. At an increasing heart rate (e.g. during an intensive muscle work), the duration of diastole decreases much more then the duration of systole.

To analyze these two phases in more detail, the cardiac cycle is usually divided into seven phases [8].

I.4.1 Atrial Contraction (Phase 1)

This is the first stage of the cardiac cycle which represents electrical depolarization of the atria. Atrial depolarization then causes contraction of the atrial musculature. As the atria contract, the pressure within the atrial chambers increases, which forces more blood flow across the open atrioventricular (AV) valves, leading to a rapid flow of blood into the ventricles. Blood does not flow back into the vena cava because of inertial effects of the venous return and because the wave of contraction through the atria moves toward the AV valve, as shown in Figure 1.6 [1]. Atrial contraction normally accounts for about 10% of left ventricular filling when a person is at rest because most of ventricular filling occurs prior to atrial contraction as blood passively flows from the pulmonary veins, into the left atrium, then into the left ventricle through the open mitral valve. At high heart rates, however, the atrial contraction may account for up to 40% of ventricular filling. The atrial contribution to ventricular filling varies inversely with duration of ventricular diastole and directly with atrial contractility [7].

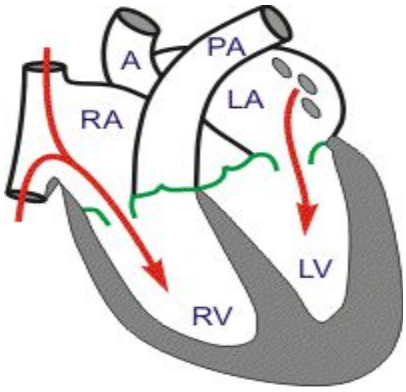

Figure 1.6 Atrial contraction.

I.4.2 Isovolumetric Contraction (Phase 2)

All Valves Closed

This phase of the cardiac cycle begins with the triggering of excitation-contraction coupling, myocyte contraction and a rapid increase in interventricular pressure. Early in this phase, the rate of pressure development becomes maximal. This is referred to as the maximal variation of the amount quantity of the movement (dP/dt) [1].

During the time period between the closure of the AV valves and the opening of the aortic and pulmonic valves, ventricular pressure rises rapidly without a change in ventricular volume (i.e. no ejection occurs).

Ventricular volume does not change because all valves are closed during this stage. Contraction, therefore, is said to be "isovolumic" or "isovolumetric". Individual myocyte contraction, however, is not necessarily isometric because individual myocyte are undergoing length changes. Therefore, ventricular chamber geometry changes considerably as the heart becomes more spheroid in shape; circumference increases and atrial base-to-apex length decreases as giving in Figure 1.7 [7].

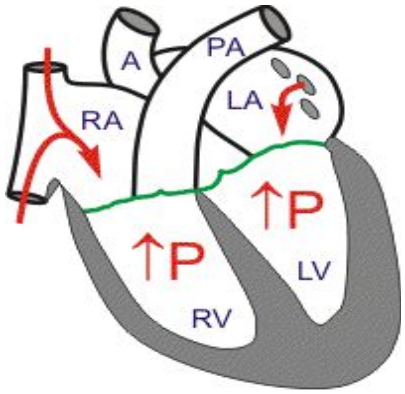

Figure 1.7 Isovolumetric contraction.

I.4.3 Rapid Ejection (Phase 3)

This phase represents the initial and rapid ejection of blood into the aorta and pulmonary arteries from the left and right ventricles, respectively. Ejection begins when the intraventricular pressures exceed the pressures within the aorta and pulmonary artery, which causes the aortic and pulmonic valves to open. Blood is ejected because the total energy of the blood within the ventricle exceeds the total energy of blood within the aorta. In other words, there is an energy gradient to propel blood into the aorta and pulmonary artery from their respective ventricles. During this stage, ventricular pressure normally exceeds outflow tract pressure by a few mmHg. This pressure gradient across the valve is ordinarily low because of the relatively large valve opening (i.e., low resistance). Maximal outflow velocity is reached early in the ejection stage, and maximal (systolic) aortic and pulmonary artery pressures are achieved [1].

Left atrial pressure initially a decrease as the atrial base is pulled downward, expanding the atrial chamber. Blood continues to flow into the atria from their respective venous inflow tracts and the atrial pressures begin to rise, and continue to rise until the AV valves open at the end of phase 5 as shown the Figure 1.8 [8].

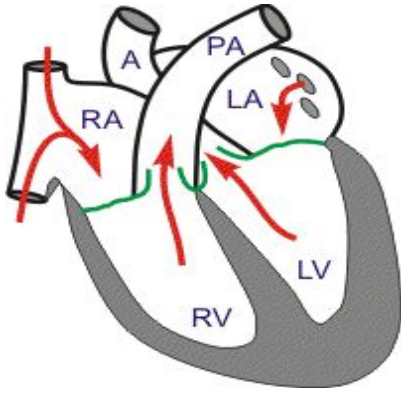

Figure 1.8 Rapid ejection.

I.4.4 Reduced Ejection (Phase 4)

Approximately 200 ms after the beginning of ventricular contraction, ventricular repolarization occurs. Repolarization leads to a decline in ventricular active tension and therefore the rate of ejection (ventricular emptying) falls [1].

Ventricular pressure falls slightly below outflow tract pressure; however, outward flow still occurs due to kinetic (or inertial) energy of the blood. Left atrial and right atrial pressures gradually rise due to continued venous return from the lungs and from the systemic circulation, respectively as shown the Figure 1.9 [7].

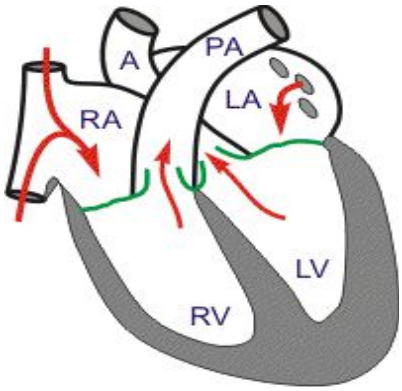

Figure 1.9 Reduced ejection.

I.4.5 Isovolumetric Relaxation (Phase 5)

All Valves Closed

When the intraventricular pressures fall sufficiently at the end of phase 4, the aortic and pulmonic valves abruptly close (aortic proceeds pulmonic). Valve closure is associated with a small backflow of blood into the ventricles and a characteristic notch the aortic and pulmonary artery pressure tracings [1].

After valve closure, the aortic and pulmonary artery pressures raise slightly following by a slow decline in pressure.

The rate of pressure decline in the ventricles is determined by the rate of relaxation of the muscle fibers, which is termed lusitropy. This relaxation is regulated largely by the sarcoplasmic reticulums that are responsible for rapidly re-sequestering calcium following contraction as given in the Figure 1.10 [7].

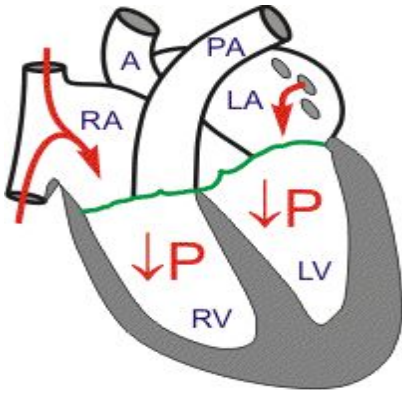

Figure 1.10 Isovolumentric relaxation.

I.4.6 Rapid Filling (Phase 6)

AV Valves Open

As the ventricles continue to relax at the end of phase 5, the intraventricular pressures will at some point fall below their respective atrial pressures. When this occurs, the AV valves rapidly open and ventricular filling begins [1]. Despite the inflow of blood from the atria, intraventricular pressure continues to briefly fall because the ventricles are still undergoing relaxation.

Once the ventricles are completely relaxed, their pressures will slowly rise as they fill with blood from the atria as given in the Figure 1.11 [7].

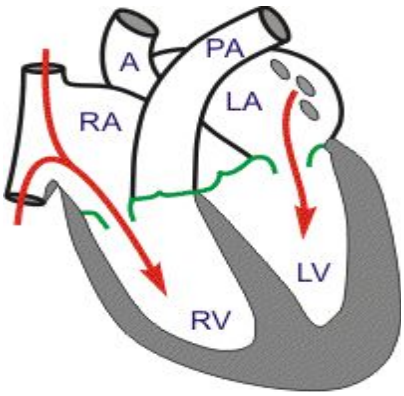

Figure 1.11 Rapid filling.

I.4.7 Reduced Filling (Phase 7)

AV Valves Open

As the ventricles continue to fill with blood and expand, they become less compliant and the intraventricular pressures rise. This reduces the pressure gradient across the AV valves so that the rate of filling falls [1].In normal resting hearts, the ventricle is about 90% filled by the end of this phase. In other words, about 90% of ventricular filling occurs before atrial contraction (phase 1) [7]. Aortic pressure and pulmonary arterial pressures continue to fall during this period as given in the Figure 1.12.

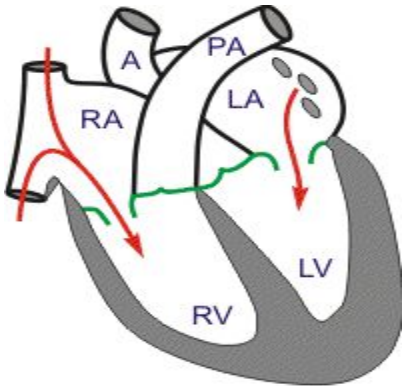

Figure 1.12 Reduced filling (diastasis).

Conclusion

The importance of the electrical activity of the heart has attracted attention of many scientists in the domain of diagnostic pathology in the myocardium due to the fact that theirs electrical activity can be the source of a wealth of valuable information on the state structure and function of the cardiovascular system, hence the need for a tool for exploring and recording the electrical activity in order to exploit it easily. Recording and representation of this electrical activity will be discussed in the next chapter.

Chapter II

The Electrocardiogram

Introduction

Electrocardiogram (ECG) is a fundamental part of cardiovascular assessment. It is an essential tool for investigating cardiac arrhythmias and is also useful in diagnosing cardiac disorders such as myocardial infarction. We present in this chapter the principle of the electrocardiogram (ECG) and its properties.

II.1 Definition

The electrocardiogram (ECG) deals with the electrical activity of the heart, which composed of series of waves ordered into some repeatable pattern. The ECG signals are obtained by connecting especially designed electrodes to the surface of the body. The height of the tracing represents millivolts while the width of the ECG represents a time interval.

The acquisition of the electrocardiogram generally consists of set of equipments which are the following:

- ✓ A set of electrodes designed to be applied in direct contact of the patient.
- ✓ An amplification system of the signals coming from the electrodes.
- ✓ A recording device.
- ✓ A system of graphic recording.

II.2 History of Electrocardiography

In 1887, the British physiologist Augustus Waller discovered it was possible to record heart activity from the skin's surface [10]. He used an instrument called a capillary electro- meter to trace heart signals onto photographic plates. Then the Dutch physiologist Willem Einthoven was inspired by Waller's experiments [11]. In 1902 he developed an instrument to record traces of the heart's activity. His string galvanometer was critical to the manufacture of early electrocardiograph machines in 1908. Early ECG machines were cumbersome and hard to use. Einthoven's first machine required five people to operate. The person monitored had to place each limb in a bucket of salt water, so it was impracti- cal for patient use. Improvements such as electrodes attached to the skin's surface meant machines became smaller, portable and

more reliable. Physiologists such as Thomas Lewis helped ECG machines gain acceptance in hospitals during the 1920 [12]. Computerised ECG machines now enable continuous heart monitoring.

II.3 Leads in ECG

In ECG recording, different electrodes detect the electrical activity of the heart and ECG recorders compare these activities. This is called “a lead”. Each lead gives a different view of the electrical activity of the heart, and so each ECG pattern will be different.

Bipolar leads use a single positive and a single negative electrode between which electrical potentials are measured. Unipolar leads have a single positive recording electrode and a combination of the other electrodes as a composite negative electrode. There are two most types of ECG recording systems; 5-leads and 12-leads [13].

In the 5-lead systems, the electrodes are properly attached with the wires labelled ‘LA’ and ‘RA’ connected to the left and right arms, and those labelled ‘LL’ and ‘RL’ to the left and right legs, respectively. They coarsely form an equilateral triangle (with the heart at the center) which is called as Einthoven's triangle. Lead I: records potentials between the left and right arm, Lead II: between the right arm and left leg, and Lead III: those between the left arm and left leg. AVL points to the left arm.AVR points to the right arm AVF points to the feet (The capital A stands for "augmented" and V for "voltage"), as shown in Figure 2.1

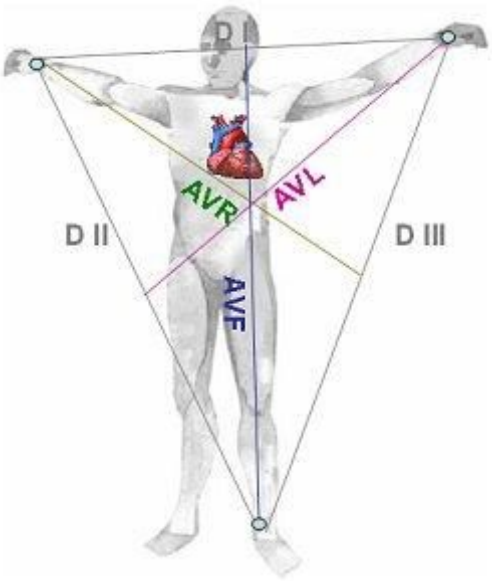

Figure 2.1 Position of Einthoven leads.

In 12-lead ECG system is the frequently used clinical ECG system and it covers the 5-lead system. It consists of 12 leads which are called I, II, III, aVR, aVL, aVF, V1, V2, V3, V4, V5, V6. Particularly, I, II, III are three bipolar leads (Einthoven leads). Three unipolar leads aVR, aVL, aVF are called Goldberger leads. Einthoven leads and Goldberger leads are positioned in the frontal plane relative to the heart as shown in Figure 2.2. Using the axial reference and these six leads (I, II, III, aVR, aVL, aVF), defining the direction of an electrical vector at a given time could be simple. Additionally, Wilson leads which are denoted by V1 - V6 are unipolar chest leads and they are placed on the left side of the thorax in a nearly horizontal plane [12], these are shown in Figure 2.3 where V1: 4th intercostal space, right sternal edge. V2: 4th intercostal space, left sternal edge. V3: between the 2nd and 4th electrodes. V4: 5th intercostal space in the midclavicular line. V5: on 5th rib, anterior axillary line. V6: in the midaxillary line.

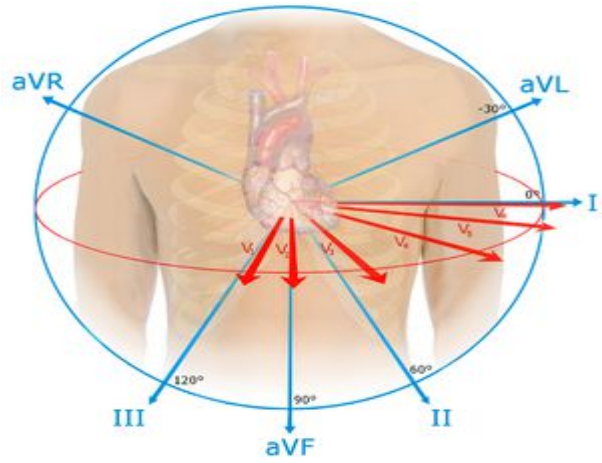

Figure 2.2 Einthoven leads and Goldberger leads position.

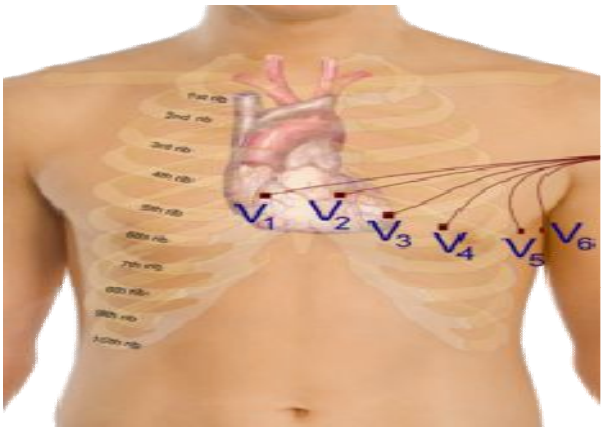

Figure 2.3 standard ECG Wilson leads position (V1, V2 ...V6).

II.4 Origin of electrical current in the heart

II.4.1 Flow of Electrical Current

As reported in the first chapter that the heart is located in the middle of the chest to the left of the mediastinum and the sinoatrial (SA) node is located in the top of the right atrium, the atrioventricular (AV) node is located in the bottom of the atrium, and the bundle branches conduct through the septum and ventricles. Because of this normal flow, the direction of the electrical flow (vector) is mainly downward, from right to left as shown in Figure 2.4 [14].

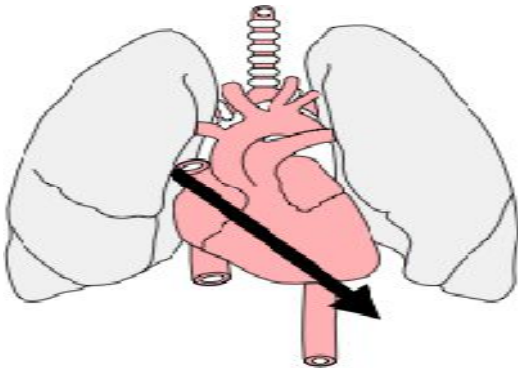

Figure 2.4 Flow of electrical current.

II.4.2 Impulse origin and atrial depolarization

When the SA node, a pacemaker cell, fires of an impulse, the impulse travels down and toward the right and left atria. The direction -or vector - of this flow is shown in Figure 2.5.The electrical flow is translated to the ECG as the P waveform is relatively small, normally between 1.5 and 2.5 mm in width and less than 3 mm in height [14].

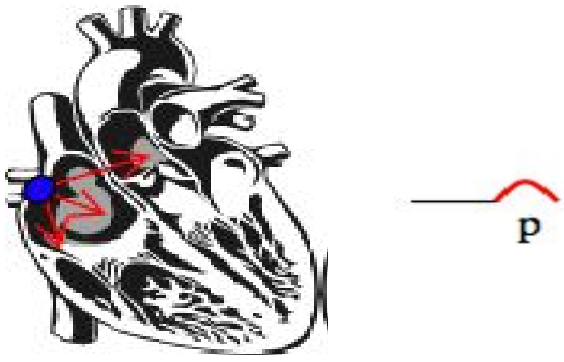

Figure 2.5 Atrial depolarization.

II.4.3 Septal depolarization

The electrical flow stops briefly at the AV node, and then travels quickly down the common bundle (Bundle of His) and through the right and left bundle branches to the interventricular septum. The depolarization of the septum causes a small negative deflection a q wave in some leads [14].

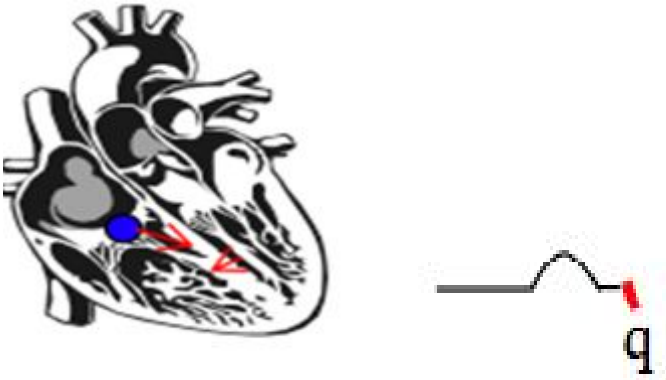

Figure 2.6 Septal depolarization.

II.4.4 Apical and early ventricular depolarization

After depolarizing the septum, the impulse moves downward and to the left. These results in a large waveform called R wave [14].

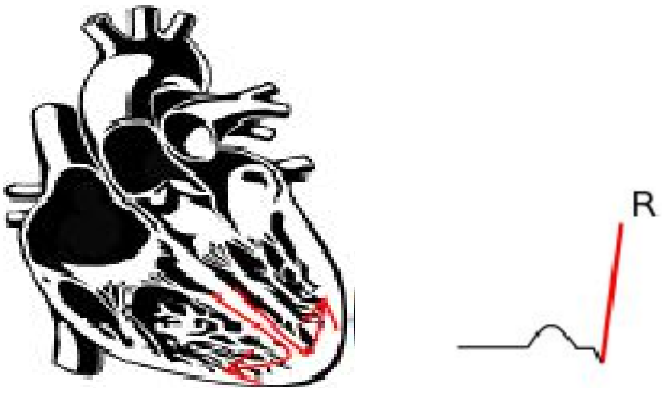

Figure 2.7 Apical and early ventricular depolarization.

II.4.5 Late ventricular depolarization

The final stage of depolarization takes place in the furthest stretches of the ventricle. The electrical stimulus moves upward, resulting in either a taller R wave or a smaller S wave [14].

Figure 2.8 Late ventricular depolarization.

II.4.6 Ventricular repolarization

Finally, the electrical stimulus is completed, ending depolarization. The ions in the cells move back into their normal resting positions, from top to bottom, causing the T wave [14].

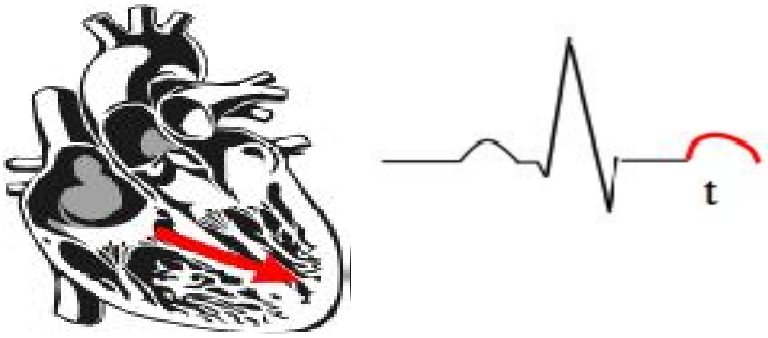

Figure 2.9 Ventricular repolarization.

II.4.7 The whole cardiac cycle

The whole results of the phases in the cardiac cycle are:

1. Atrial depolarization (P wave).
2. Septal depolarization (Q wave).
3. Early ventricular depolarization (R).
4. Late ventricular depolarization (S wave).
5. Ventricular repolarization (T wave).

Figure 2.10 The whole cardiac cycle.

II.5 The ECG components

The ECG signal consists of waves, intervals and segments. The three basic waves are P, QRS and T. These waves correspond to the far field induced by specific electrical on the cardiac surface. In a representation of normal ECG waveform generally are:

•A wave is every deflection on the ECG.

• A segment is the region between two waves.

• An interval includes one segment and one or more waves.

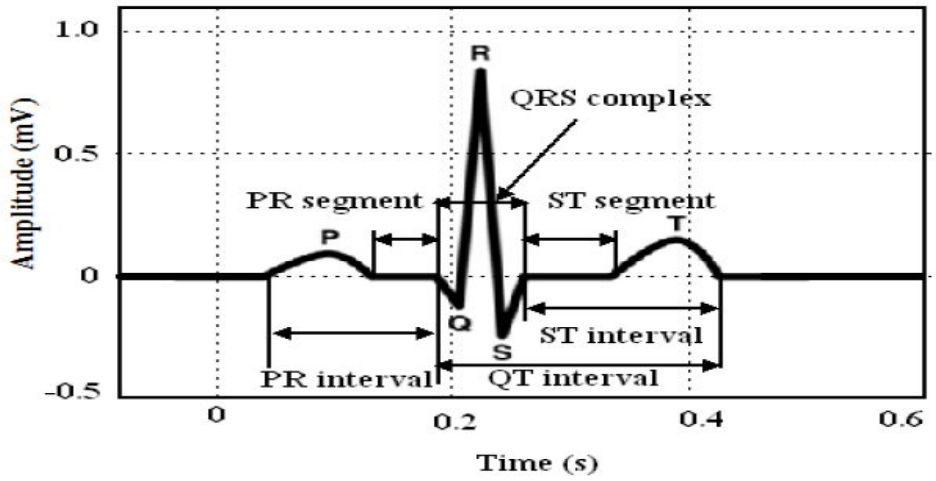

Figure 2.11 Schematic representation of normal ECG waveform.

The polarity and the shape of the ECG constituent waves are different depending on lead that is used. Usually ECG signals are contaminated by various kinds of noise. Various types of noise contaminated the ECG are described in the next passage.

I.5.1 The Isoelectric Line (baseline)

There is a part of the normal ECG rhythm that is electrically neutral there is nothing electrically happening in the heart during that period. This is called the “isoelectric” line. This is a straight line passing from the end of the T wave and the beginning of the next P wave this is shown in Figure 2.12.

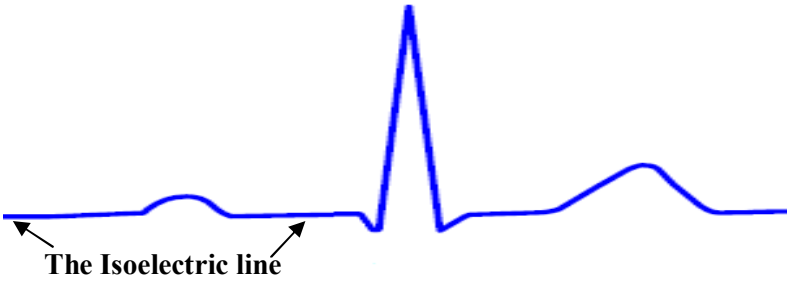

Figure 2.12 Baseline or Isoelectric Line.

II.5.2 The P wave

The P wave on the ECG signal , marks the depolarization and contraction of the right and left atria , the amplitude level of this voltage signal wave is low (approximately 1 mV) [15].

Figure 2.13 P wave.

II.5.3 The PR segment

The PR segment is the line between the end of the P wave and the beginning of the QRS complex. The PR segment signifies the time taken to conduct through the slow AV junction. This delay allows for atrial kick [15].

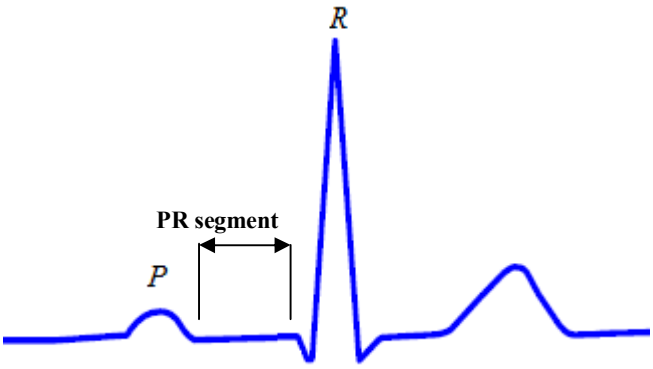

Figure 2.14 The PR segment

II.5.4 The PR interval

The PR interval is measured from the start of the P wave to the start of the QRS complex. While it might appear obvious that this is indeed a PQ interval, a Q wave is not always present on an ECG tracing. For consistency, the term is PR interval has been adopted whether a Q wave exists or not [15].

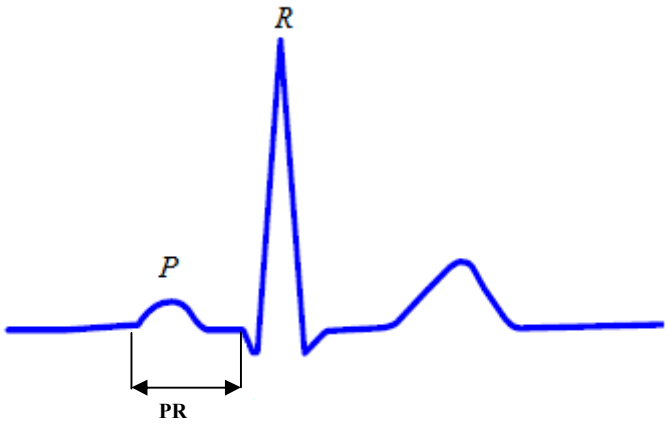

Figure 2.15 The PR Interval.

II. 5.5 The QRS complex

The QRS complex is the largest voltage deflection of approximately 10–20 mV but may vary in size depending on age, and gender. The voltage amplitude of QRS complex may also give information about the cardiac disease [13]. Duration of the QRS complex indicates the time for the ventricles to depolarize and may give information about conduction problems in the ventricles such as bundle branch block. The normal depolarization of the ventricles is illustrated in Figure 2.16.

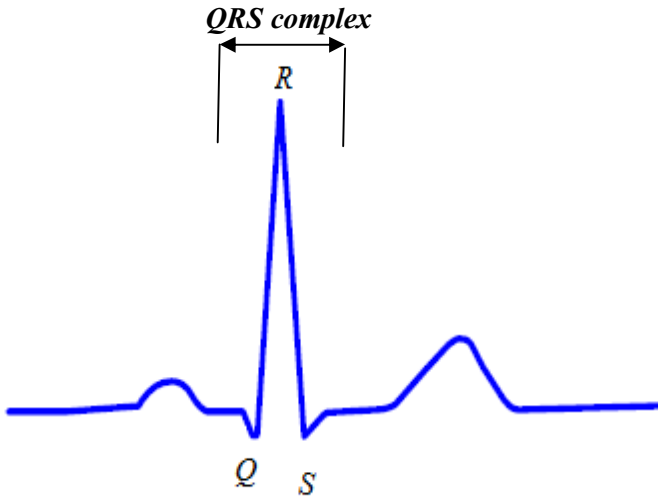

Figure 2.16 The QRS complex.

Three distinct waveforms are often present in a normal QRS complex representing ventricular depolarization. Depolarization of the ventricular septum begins first from left part of the heart to the right. This early depolarization causes a small downward deflection called a Q wave. A Q wave is the first negative deflection of the QRS complex that is not preceded by a R wave. A normal Q wave is narrow and small in amplitude.

Following the depolarization of the interventricular septum, an R wave is the first positive deflection of the QRS complex., an S wave is the first wave after the R wave that dips below the baseline (isoelectric line) [15]. Various QRS Complex morphologies are represented in Figure 2.17.

.

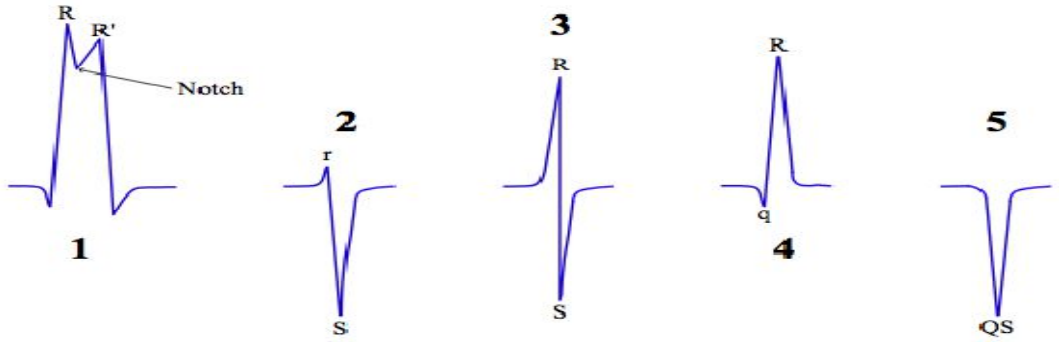

Figure 2.17 Various QRS complex Morphologies

As a convention all these different morphologies are defined as QRS complexes as shown in the figure2.17 [15] the classification of each one are:

- QRS-1 demonstrates the labelling convention for subsequent positive deflections above the baseline after the R wave. This second deflection is labelled R'. Note that a third upright deflection would be labelled R'' (R double prime).
- QRS complex -2-4 are all normal QRS complexes of different shapes.
- QRS complex -3 is a biphasic QRS complex would be labelled RS.
- The QRS complex -5 is a QS complex.

II.5.6 R-R interval

The RR interval is the time between QRS complexes as shows Figure 2.18. The instantaneous heart rate can be calculated from the time between any two QRS complexes. The drawback of this method is that the calculated heart rate can be quite a bit different from the measured pulse even in a normal person due to variations in the heart rate associated with respiration (the sinus arrhythmia).

II.5.7 The T wave

A T wave usually follows every QRS complex. The T wave corresponds to the repolarisation of the ventricle. While ventricular depolarization occurs rapidly producing a tall QRS complex, ventricular repolarisation is spread over a longer interval, resulting in a shorter and broader T wave as shows Figure 2.19. Abnormally shaped T waves can indicate acute cardiac ischemia, electrolyte imbalances, and cardiac disease related medication [15].

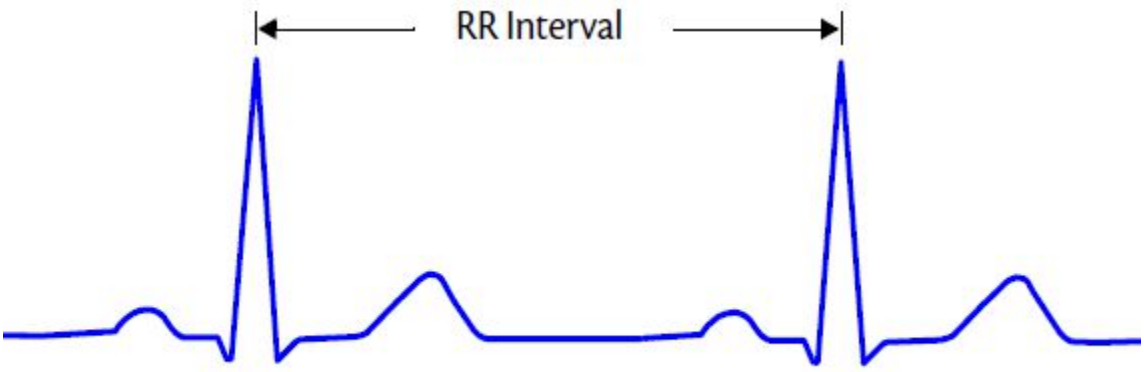

Figure 2.18 R-R interval

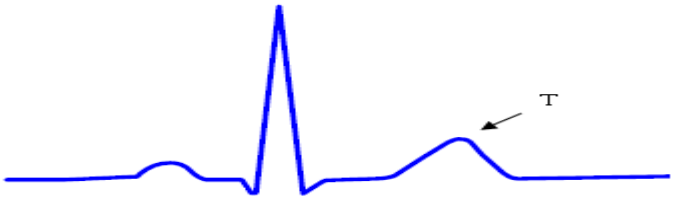

Figure 2.19 T wave

II.5.8 The U wave

Occasionally, another wave, the U wave, is recorded immediately following the T wave and before the P wave. The U wave has yet to be fully explained but current studies suggest it represents a final stage of repolarisation of certain ventricular cells in the middle of the myocardium. The U wave will most often be oriented in the same direction as the T wave [15]

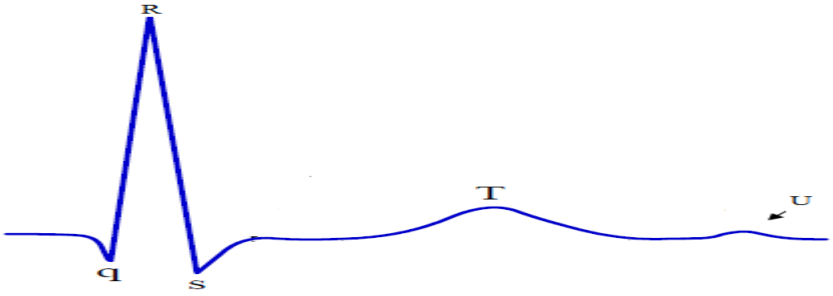

Figure 2.20 U wave

II.6 Noises in ECG Signal

Generally the recorded ECG signal suffer from noises originating from various sources and artifacts that can be within the frequency band of ECG signal, which may change the characteristics of ECG signal. Hence it is difficult to extract useful information of the signal. The corruption of ECG signal is due to following major noises.

II.6.1 Power line interferences

It is produced due to environment of experiment where it is surrounded by electromagnetic waves. Its frequency range is 50-60Hz with some random initial phase. A 60 Hz notch filter can be used remove the power line interferences [16].

II.6.2 Baseline drift

Baseline drift may be caused in chest-lead ECG signals by coughing or breathing with large movement of the chest, or when an arm or leg is moved in the case of limb-lead ECG acquisition [16]. Base-line drift can sometimes caused by variations in temperature and bias in the instrumentation and amplifiers. Its frequency range generally 0.5Hz. To remove baseline drift a high pass filter with cut-off frequency 0.5Hz is used [16].

II.6.3 Movement artifacts

Motion artifacts are transient baseline change due to electrode skin impedance with electrode motion. It can generate larger amplitude signal in ECG waveform [10]. The peak amplitude of this artifact is 500 percent of Peak to Peak ECG amplitude and its duration is about 100–500 ms [12]. An adaptive filter can be used to remove the interference of motion artifacts.

II.6.4 Muscle contraction (EMG)

The EMG is caused by muscular contraction, which generates microvolt-range electrical signal. Such physiological interference may be minimized by strict instructions and self-control. EMG noise is assumed to be zero mean Gaussian noise.

II.7 Steps in ECG Analysis

The major steps in the analysis of the ECG signals are:

- Noise elimination from ECG using noise filter technique.
- Cardiac cycle detection by detecting QRS complex.
- Detection of significant characteristic points in ECG signal.
- Formulation of characteristic feature set.

Conclusion

In classical clinical routine faced a problem in diagnostic of the ECG signal, we mean the QRS complex waves detection is done in manual fashion. In general, this is acceptable when the length of the ECG signal is small witch is not the case in the most of the situation .In order to overcome this problem Pan and Tompkins propose a solution to extract automatically the QRS complex from the ECG signal . The different steps of this algorithm will be explained in the next chapter.

Chapter III

Algorithm of Detection

Introduction

The detection of QRS complex is the first step towards automated computer-based ECG signal analysis. All the required features from ECG are extracted from the filtered ECG signal. The basic and essential component for feature extraction is the detection of the QRS complex i.e. locating the R peak for each beat of the signal. Once the R peak is determined, all other characteristic peaks on the ECG signal are determined with reference to the R peak. Thus an accurate detection of the QRS complex of the ECG signal is a crucial task in ECG analysis [18]. In the literature several techniques are reported to improve the accuracy of QRS complex detection from the ECG signal because the exact detection of QRS complex is difficult, as the ECG signal is contaminated with different types of noise like electrode motion, power-line interferences, baseline wander, muscles noise etc. [19]. Pan and Tompkins pioneered a technique where, the detection of QRS complex was achieved by linear filtering, non-linear transformation and decision rule algorithm [20]. In another method the QRS complex of the ECG signal was found out using multi rate signal processing and filter banks [21]. The QRS complex can be found after finding the R-peak by differential operation in ECG signal. The first differentiation of ECG signal and its Hilbert transform is used to find the location of R-peak in the ECG signal [22].

III.1 Structure of the QRS detection algorithm

The majority of the proposed algorithms to process the problem of the automatic QRS detection in the ECG signals, they share the same common structure. We can say that they are based on two stage steps, the first phase is the preprocessing stage of the ECG signal and the second phase is Decision stage. The common scheme is shown in the following Figure.

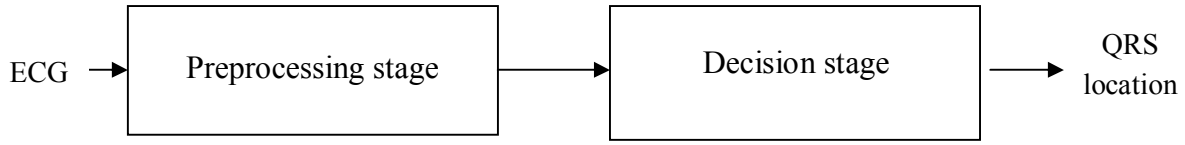

Figure 3.1 The common structure of the QRS detectors.

The preprocessing stage generally for the ECG signal is to automate the analysis of noises present in signal are needed to be considered and eliminated for the accurate signal analysis and diagnosis. Electrocardiogram (ECG) can be corrupted by various types of noise such as power line interference, electrode contact noise, motion artifacts, EMG noise, instrumentation noise, wandering baseline as described in chapter II. The ECG signal embedded in these noises is very hard to correctly interpret for diagnosis. To obtain a distortion less, accurate and error free signals several filters technique are using.

Decision stage is the final step in the QRS detection algorithm, different methods are used to extract correctly the location of the R peaks in the ECG signal. The majority of algorithms use the adaptive thresholding [23].

III.2 The ECG signal filtering

The filtering techniques are primarily used for preprocessing of the ECG signal and have been implemented in a wide variety of systems for ECG analysis. To reduce and remove the noises, digital software filters are widely used in biomedical signal processing [24].

Analog filters can deal with the noises, but they introduce nonlinear phase shifts and depend on the instrumentation such as resistance, temperature and design. Analogue filter characteristics are typically fixed by the circuit design and component values. If we wish to change the filter characteristics we would have to make major modifications to the circuit. In comparison digital filters characteristics can be changed very easily by simply changing the algorithm embedded into the processor. Digital filters are more precise and less error with more advantages over analog filters. Filters have two uses: signal separation and signal restoration. Signal separation is needed when a signal has been contaminated with interference, noise, or other signals. For example, imagine a device for measuring the electrical activity of a baby's heart (EKG) while still in the womb. The raw signal will likely be corrupted by the breathing and heartbeat of the mother. A filter might be used to separate these signals so that they can be individually analysed [17].

Digital filters are classified either as Finite Impulse Response (FIR) filters or Infinite Impulse response (IIR) filters, depending on the form of unit pulse response of the system. In the FIR system, the impulse response is of finite duration whereas in the IIR system, the impulse response is of infinite duration. IIR filters are usually implemented using structures having feedback, that's why the present response of IIR filter is a function of present and past values of the excitation as well as the past value of the response. But the response of the FIR filter usually implemented using structures having no feedback so the response depends only on the present and past values of the input only [16].

III.2.1 Design Techniques of FIR and IIR Filters

The FIR filter is implemented in a non-recursive way which guarantees a stable filter. FIR filter design mainly consists of two parts:

- Approximation part
- Realization part

In the approximation stage, the specifications of the filters are taken and a transfer function is generated. In approximation, first an ideal frequency response is taken of length *N* (*N* represents the order of the FIR filter). Then a method or algorithm is selected for the implementation of the filter transfer function.

In the realization part, a structure is chosen to implement the transfer function i.e. in the form of circuit diagram or a program. There are essentially three well-known methods for FIR filter design namely:

- The window method
- The frequency sampling technique
- Fourier series method

The equations below show the input output relation of the filter and transfer function of the FIR filter:

$$y[n] = \sum_{k=0}^{N-1} b_k \, . x[n-k] \tag{3.1}$$

The first filter designed for the task of removing the noise from original signal is an FIR filter. A filter lends itself quite well to this task considering that we are interested in removing a very specific, narrow band of frequencies [25].

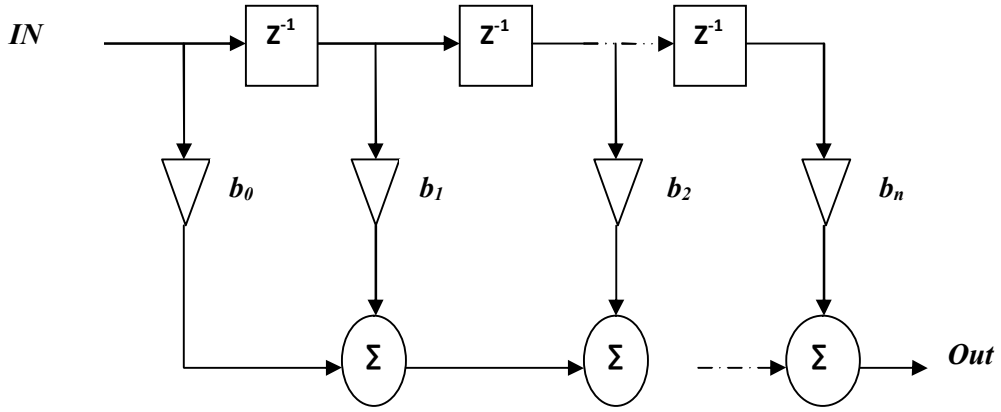

Figure 3.2 FIR Filter Structure

The center frequency of the filter, F_0 was chosen to be at exactly 60Hz and the bandwidth ΔF=4Hz.

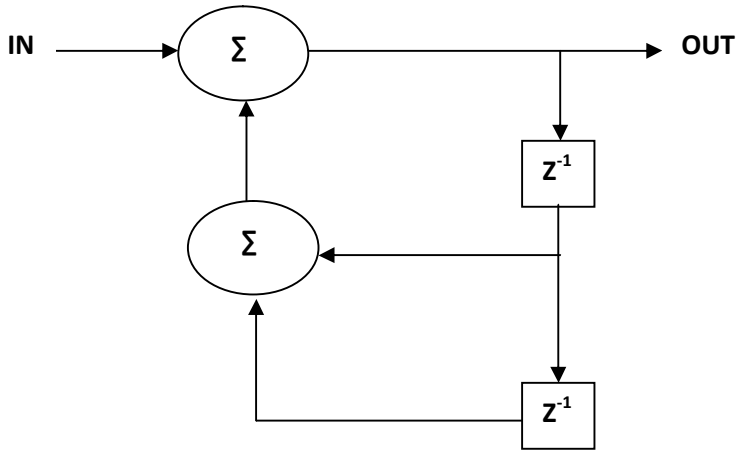

Figure 3.3 IIR Filter Structure

An IIR filter offers the very best of what FIR filters have to offer; very high attenuation with a low order. The filter presented is of order two and has only one coefficient. These properties lend themselves to being a light computational load [26].

III.2.2 A comparison between IIR and FIR filters

IIR filters are not linear phase filters there is severe phase shift around the stop band of the filter. This could pose a problem for this application given the importance of maintaining meaningful timing data. After all, the physician is primarily concerned with the time at which different peaks and waves occur at within the ECG. After closely examining an IIR filter and FIR filters of varying order, we found the IIR to perform best overall [29]. Although the IIR filter's phase response is non-linear, almost all of the non-linearity occurs within the FIR filter. This would seem to indicate that it's shifting the phase of frequencies we're not interested in anyway. The IIR's low computation cost is also of importance especially if you're looking at implementing some sort of noise filter for an actual piece of medical equipment. This implies finite computational resources and keeping costs down. The IIR filter achieves both of these goals while still delivering a high quality filtered signal [27].

The comparison of the two filters show that the IIR filter is much better than the FIR filter in the preprocessing technique. Noises and artifacts play a vital role in the processing of ECG signal. It becomes difficult for the physicians to diagnose the diseases if the artifacts are present in the ECG signal. For artifacts like power line interference, digital filters were implemented and the amplitude spectra were compared for the evaluation of their performance. FIR filters have important property of linear phase. This property plays a main role for ECG signal analysis. In addition, the mean square error is estimated for the performance of digital filters quantitatively. The mean square error of IIR filter is lower than that of FIR digital filter. Therefore, due to the low computational cost of IIR filter, the IIR filter is suitable for the real-time implementation in hardware. For the baseline wonder removal due to its lower frequency characteristics, FIR and IIR high-pass filters were implemented. The performance of the filter was up to an acceptable extent and no information of ECG signal was lost during analysis. FIR filters are preferred for ECG signal processing due to the property of linear phase but the major drawback is the higher orders of filters are required and the signal was delayed proportionally to the orders of filter. IIR filters need only a few filter orders at the same time less hardware is required and complexity and computational cost is reduced .On the basis of above discussion it is found that IIR filters can be preferred over FIR filter [35].

.

III.3 State of the art

Several algorithms are available in order to detect automatically the QRS complex or over specifically the R wave which enable further to characterise the heart rate and the current state of the heart. The majority of the algorithms are used the procedure based on signal derivatives and thresholding. Each algorithm has its advantages and inconveniences such as the robustness, complexity, and the computing cost, the degree of sensitivity to noise and the disturbances of the baseline. Within the last three decades many new approaches have been proposed for example, algorithms from the field of the artificial neural network, genetic algorithms, and wavelet transform and filter banks. In the next section we give an overview about the stat of the art of the major algorithms in the domain of QRS detection in ECG signal, we use the same chronology used in [34].

The Previous works were fundamentally use a very simple models based linear or non-linear filter or filter banks methods (Okada, 1979; Afonso, 1999). These methods require less computation power and are most suitable for in embedded real-time monitoring applications. The inconvenience is that the precision of the QRS feature extraction is limited as the processing involves only selected range of frequencies of the ECG signals.

In fact the majority of the proposed methods in the literature utilise the derivative methods with thresholding to discriminate between the R wave and other waves.

A QRS complex detection scheme evolved by Fraden and Neuman (1980), in this method they calculated the threshold as a fraction of the peak value of the ECG. In 1985, Pan and Tompkins proposed an algorithm (the so-called PT method) to recognize QRS complex in which they analyzed the locations and magnitudes of several waves (R waves) and to reduce the false detection of ECG signals they used a special digital band pass filter (BPF). The first step in their algorithm is to use a digital band pass filter to eliminate all the high frequency and to reduces false detections caused by the various types of interference present in ECG signals, in the next step they differentiated the filtered signal to get information about the slope of the QRS complex, squared step it used to amplify the output of derivation stage and finally computed integral of each moving window to quantify QRS and non-QRS. And thresholding is done for both band pass and integrated signal to improve the reliability of the QRS detection.

In 1995 Li *et al.* proposed a method based on finding the modulus maxima larger than a threshold obtained from the pre-processing of preselected initial beats. In Li *et al*. method, the threshold is updated during the analysis to obtain a better performance. This method has a post-processing phase in which redundant R waves or noise peaks are removed. The algorithm

achieves a good performance with a reported sensitivity of 99.90% and positive prediction value of 99.94% when tested on the MIT/BIH database.

QRS complex detection algorithms based on wavelet transform are also widely examined (1995; Li *et.* 1993; Sahambi *et al*. 1997; Mahmoodabadi *et al*. 2005; Sasikala *et al*. 2010; Bsoul *et al*.2009). With the wavelet based analysis, each QRS complex corresponds to a couple of maximum and minimum in wavelet transform. In the analysis by wavelet using different scales in time-and frequency-domain the signals are divided into different response clusters which represent different frequency components of the ECG.

In order to filter and analyze ECG signals Kozakevicius *et al.* (1988) utilized orthogonal wavelets. They used succinctly supported wavelets associated to the statistical Stein's unbiased risk estimator in order to obtain an adaptive thresholding strategy to filter ECG signals and then they analyzed the filtered signals by using the Haar wavelet transform in order to detect the locations of the occurrence of the QRS complex during the period of analysis.

A QRS complex detector method based on the dyadic wavelet transform (DWT) was described by Kadambe *et al.* (1999), which was robust to time-varying QRS complex morphology and to noise. They designed a spline wavelet that was suitable for QRS detection, where scales of this wavelet were chosen based on the spectral characteristics of the ECG signal. They performed their QRS detection algorithm upon American Heart Association (AHA) data base and the algorithm have different performances with an error of 0.2% - 15.4% for different ECG records. Another QRS complex detection algorithm implemented using the wavelet by Szilagyi *et al.* (2001) that could be applied in various on-line ECG processing systems. In the first step the objective is to eliminate the low pass and high pass frequency components for this reason they filtered the signal with wavelet transform, following by a second step based wavelet transform in which they obtain a few maxima and minima in each period of the transformed signal and detected the extreme values. To determine the location of the R peaks they use a strategy: The peaks which came before a long ascent and followed by a long descent of the signal are offered R peaks. They tested the algorithm to MIT-BIH database and had detection ratio about 98.9% .

Legarreta *et al.* (2005) have extended the work of Li *et al*. utilizing the continuous wavelet transform (CWT). Their CWT based algorithm affords high time–frequency resolution which provides a better definition of the QRS modulus maxima curves. This allows them to follow QRS wave across scales in noisy signals, and better define the spectral region corresponding to the QRS maxima peak. They tested the algorithm using patient signals recorded in the Coronary Care Unit of the Royal Infirmary of Edinburgh with a positive predictive value

of 99.73% and with the MIT/BIH database obtaining a positive predictive value of 99.68%. In 2006, S.A.Choukari *et al.* for detecting QRS complex, they used different decomposition level wavelet coefficients to detecting P and T waves and by combining of them they obtained the denoised ECG signal. They compared the performance of their algorithm with db5, db10, coif5, sym6, sym8, biorth5.5 by calculating MSE (mean squared error) and PSNR (Peak Signal to Noise Ratio). The importance of the proper selection of mother wavelet with appropriate number of decomposition levels attract attention to M.Kania *et al.* they studied this for reducing the noise from the ECG signal. The authors claimed that they obtained good quality signal for the wavelet db1 at first and fourth level of decomposition and sym3 for fourth level of decomposition. In 2008 an algorithm called R-point detector proposed and implemented by Rizzi *et al.* based adaptation of fast parallelized wavelet transforms for the detection of R-wave in the presence of different types of noises. The algorithm gave high degree of noise immunity and predictivity. To detect QRS complexes, in general researchers used some known wavelet functions Ktata *et al.* (2006) used Daubechies 1 wavelet to produce an algorithm for detecting not only QRS complex but P wave and R wave. They decomposes the ECG signal into five levels by using continuous wavelet, to obtain the scalogram of ECG and the detection of R peaks is reached from level number one but the detection of T wave and P wave is reached from level four and five. They used a rectangular window centered in the maxima detected for each wave to make a truncation and then mark-up the ECG signal by maximum detected .Daqrouq *et al.* (2008) used Symlet as a wavelet function. Their detector was based on using the CWT with sym8 and scale 2^3. They applied the Mallat's algorithm to calculate the wavelet approximation coefficients and then they computed the square of coefficients to specify a threshold level for detecting the maximum in every window, which indicated the R peaks. They also computed the R-R interval and heart rate. The average rate of QRS detector achieved is about 99.75 using MIT/BHI data base. In 2008, Rizzi *et al.* proposed and implemented an algorithm called R-point detector based on adaptation of fast parallelized wavelet transforms for the detection of R-wave in the presence of different types of noises. They selected the bior 3.3 wavelet as a mother wavelet because of its similar shape to a QRS complex. They applied soft thresholding technique into dyadic scales and decomposed the ECG signal. They evaluated the algorithm to MIT/BIH Noise Stress Test Database with a 99.6% detection success. In 2010, Elgendi *et al.* used Coiflet as a wavelet function. Their algorithm using an adaptive threshold based on an approximation of Peak Signal to Noise Ratio (PSNR) was developed to detect QRS complexes in arrhythmia ECG Signals that suffer from non-stationary effects, low PSNR, negative QRS polarities, low QRS amplitudes and ventricular ectopic. Their method was tested on MIT/BIH Arrhythmia Database with 98.2%

average success of true detective QRS complex. An ECG feature extraction system based on multi resolution Wavelet Transform was developed in 2010 by Karpagachelvi *et al*. The first step in their algorithm based to denoise the ECG signal by Discrete Wavelet Transform using Haar wavelet, in the next step they detected the R peaks which are over the threshold level. They examined the performance of the R-peaks detector by testing their algorithm on the standardized MIT/BIH database.

There are in addition of the methods used derivative technique and wavelet decomposition other methods which are summarized in the following paragraphs.

Martinez *et al.* (2004) use an algorithm to detect QRS based on the characteristic in the ECG signal that QRS complexes have more energy and higher amplitude and maxima lines over a longer frequency interval, and P and T waves have less energy and lower amplitude and maxima lines over a shorter frequency interval. The QRS components also have a different shape from the rest of the ECG waveform; a difference that enables simple QRS detection. In 2006 Chawla *et al.* proposed an algorithm to detect QRS complex in the ECG signal using Principle Component Analysis as a signal expansion method. They created eigenvectors which form a new orthogonal basis finding various segments of an ECG waveform and they used Fast Fourier Transform for the results and extracted the QRS complex portion and excluded P-wave and T-wave.

Hilbert transform method also was used in first time in 1988 by Zhou *et al.* Then, In 2000 Benitez *et al.* proposed an algorithm for detecting QRS using Hilbert Transform. They used a moving 1024 points rectangular window to subdivide the signal, differentiated them and performed the Hilbert Transform. They applied an adaptive threshold level to Hilbert sequence to detect the R peaks. When two detected R peaks are very close each other (less than 200 ms), only one of them is selected as the R peak. They tested their algorithm upon MIT/BIH Arrhythmia database with QRS detection error rate of 0.36%. Oliveria and Cortez (2004) used Hilbert transform pairs of wavelet bases in order to develop pass band filter between 5-40Hz to emphasize the R wave peaks and they determined the RR intervals from that signal. Neural Network applications were also used for QRS detection. Viyaja *et al.* (1997) used predictive Neural Network based technique. They trained the Network for two classes; QRS and non-QRS using the back propagation algorithm predict the QRS from the ECG signal. In 2009, Abibullaev & Hee Don Seo implemented a method for detection and classification of QRS complexes in ECG signals using continuous wavelets and Neural Networks. Firstly they analyzed ECG by using dB5, sym4, bior 1.3 and bior 6.8 wavelets, then they employed these wavelets as the mother wavelet, applied continuous Wavelet Transform decomposition. Second step based to

determine an adaptive threshold level and handled few wavelet coefficients after thresholding. Finally they used three layer feed forward Networks with back propagation learning algorithm. They evaluated their algorithm using arrhythmic ECG data from the American Heart Association (AHA) database with an average accuracy of 95.78%. In 2010 R.S.D. Wahidabanu and P. Sasikala developed an algorithm for a robust QRS detection using Discrete Wavelet Transform (DWT). This transform provides efficient localization in both time and frequency. Analysis is carried out using MATLAB Software. The correct detection rate of the Peaks is up to 99% based on MIT/BIH ECG database. Also using the wavelet transform, in April 2012, S. Banerjee et al implemented an algorithm of QRS detection, in which they utilise multiresolution wavelet analysis method. The Denoising step is performed by discarding detailed coefficients D1 and D2,then the QRS zone is selected by D4 + D5 and adaptive thresholding. The Fiducial points are determined by amplitude and slope reversal point detection. The Average sensitivity and predictivity of 99.8% and 99.6% with MIT/BIH database obtained.

Xue *et al.* (1992), Cohen *et al.* (1995), Tan *et al.* (2000) also studied Neural Networks Algorithms. The Neural Network Algorithm has a large utilization in ECG classifier of normal and abnormal beat in the last five years.

III.4 Adapted solution

III.4.1 Pan and Tompkins Algorithm methods

Pan and Tompkins proposed a real time QRS detection algorithm in 1985 [20]. It recognizes QRS complexes based on analyses of the slope, amplitude, and width. Figure 3.4 shows the various processing steps performing the analysis of the ECG signal.

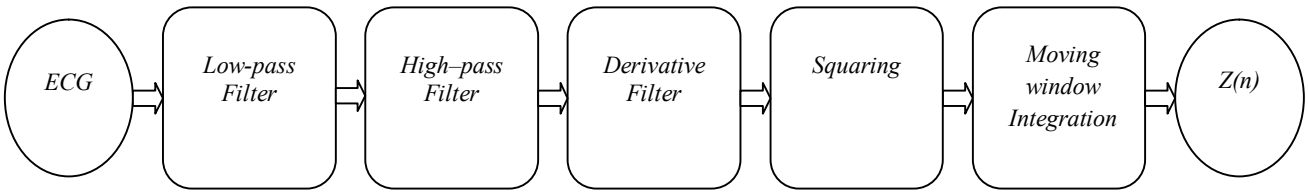

Figure 3.4 Block filter stages of the QRS detector using pan and Tompkins algorithm
ECG is the input signal; z (n) is the time-averaged signal.

The first step is a band pass filter composed of cascaded low pass and high pass that require only integer coefficients. Its function is to isolate the predominant QRS energy centred at 10 Hz, attenuates the low frequencies characteristic of P and T waves and base line drift. The next step

of the processing is differentiation, this step is required in order to emphasize the high slope of the QRS complex following by a non linear transformation that consist of point by point squaring of the signal, This transformation serves to make all the data positive. Next the squared waveform passes through a moving window integrator; it's used to ensure that a measure of QRS complex width is included in the processed signal. They chose the window's width to be long enough to include the time duration of the extended abnormal QRS complexes, but short enough to include T wave. In their work they take the width of the window equal to 30 samples.

Adaptive amplitude thresholds applied to the band pass filter wave form and the moving window integration wave form are based on continuously adapted estimates of the peak signal level and peak noise. After preliminary detection by the adaptive thresholds, decision processes make the final determination as to whether or not a detected event was a QRS complex. in the following sections we will describe in more details of the precedent stage:

III.4.2 The bandpass filter

The bandpass filter for the algorithm of Pan and Tompkins reduces the noise in the ECG signal by matching the spectrum of the average QRS complex. Thus it attenuates baseline drift, and T wave interference. The bandpass filter maximizes the QRS energy is approximately in 5-15 Hz [28], [29]. The filter implement in this algorithm is a recursive integer filter in which poles are located to cancel the zeros on the unit circle of the Z plan [30]. A low pass filter and high pass filter are cascaded to form the bandpass filter.

III.4.2.1 Low pass filter

The transfer function of the second-order low-pass filter is:

$$H(z) = \frac{(1-z^{-6})^2}{(1-z^{-1})^2} \tag{3.2}$$

$$H(Z) = \frac{Y(Z)}{X(Z)} = \frac{(1-z^{-6})^2}{(1-z^{-1})^2} \tag{3.3}$$

$$Y(Z)(1-z^{-1})^2 = X(Z)((1-z^{-6})^2 \tag{3.4}$$

The difference equation of this filter after applied the inverse Z transform is:

$$y(nT) = 2y(nT - T) - y(nT - 2T) + x(nT) - 2x(nT - 6T) + x(nT - 12T) \tag{3.5}$$

Where the cut-off frequency is about 11 Hz and the gain is 32. The filter processing delay is six samples. In order to avoid saturation the output of the filter is divided by 32 [31].

The performances of this filter are:

- 1-Linear phase response.
- 2-Attenuation of the frequency of 60 Hz (noise of interference).
- 3-Attenuation of all high frequency.

The performance of the low-pass filter shows by the figure 3.5 .This filter has purely linear phase response. Therefore, power line noise is significantly attenuated by this filter. Which represent attenuation of the frequency in -35 dB belong to the interval [0.3 f/fs.0.35f/fs].Since the sample rate is 200 sps for these filters, this represents a frequency of 60 Hz. Also all higher frequencies are attenuated by more than 25 dB.

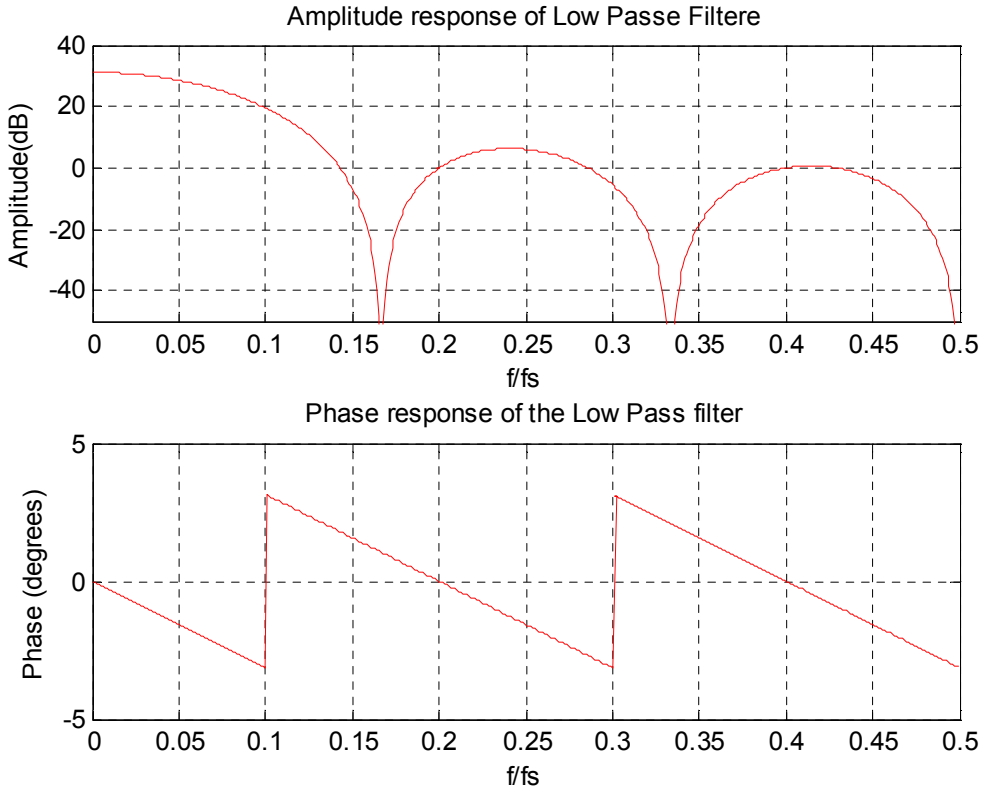

Figure 3.5 Amplitude response; Phase response of the low-pass filter.

III.4.2.2 High pass filter

The design of the high-pass filter is obtained by dividing the output of the first order low-pass filter by its gain and then subtracting from an all-pass filter with delay.

The low-pass filter is an integer-coefficient filter with the transfer function is:

$$H_{lp}(Z) = \frac{(1-Z^{-32})}{(1-Z^{-1})} \tag{3.6}$$

Where the equation (3.6) can be put in the following form:

$$H_{lp} = \frac{Y_{lp}(z)}{X_{lp}(z)} = \frac{(1-Z^{-32})}{(1-Z^{-1})} \tag{3.7}$$

$$Y(z)_{lp}(1 - Z^{-1}) = X(z)_{lp}(1 - Z^{-32}) \tag{3.8}$$

After applying the inverse Z transform the difference equation of the filter is given flow:

$$y(nT) = y(nT - T) + x(nT) - x(nT - 32T) \tag{3.9}$$

This filter has a dc gain of 32 and a delay of 15.5 samples.

Before subtracting the original signal is delayed by 16 T (i.e. Z^{-16}) to compensate for the low-pass delay (All-pass filter) [29].

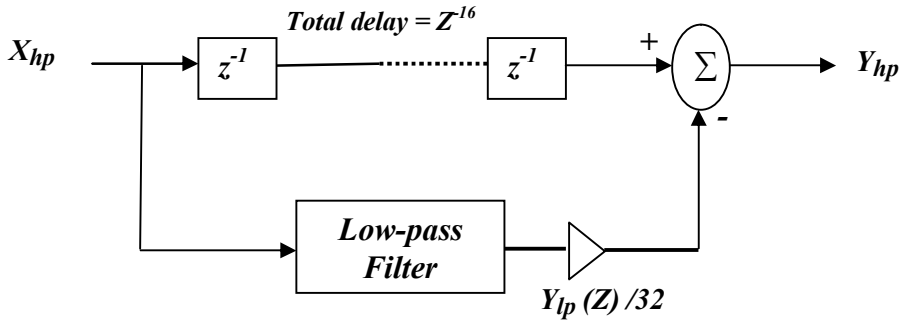

Figure 3.6 The high-pass filter is implemented by subtracting a low-pass filter from an all-pass filter with delay.

The transfer function of the high-pass filter is :

$$H_{hp}(Z) = \frac{Y_{hp}(Z)}{X_{hp}(Z)} = Z^{-16} - \frac{H_{lp}(Z)}{32} \tag{3.10}$$

$$H_{hp}(Z) = \frac{-1+32\,Z^{-16}-32\,Z^{-17}+Z^{-32}}{32(1-Z^{-1})} \tag{3.11}$$

$$H_{hp}(Z) = \frac{Y_{hp}(Z)}{X_{hp}(Z)} = \frac{-1+32\,Z^{-16}-32\,Z^{-17}+Z^{-32}}{32(1-Z^{-1})} \tag{3.12}$$

After devlopping the equation (3.12) we obtain :

$$Y_{hp}(Z)\ 32(1 - Z^{-1}) = X_{hp}(Z)\ (-1 + 32\ Z^{-16} - 32\ Z^{-17} + Z^{-32}) \qquad (3.13)$$

And the difference equation of the filter is obtained by the inverse Z transform:

$$y(nT) = y(nT - T) - \frac{x(nT)}{32} + x(nT - 16T) - x(nT - 17T) + x(nT - 32T)/32 \qquad (3.14)$$

The low cut-off frequency of this filter is about 5 Hz, and the gain is one. This filter has a delay of about 16T (80 ms) [29].The Figure 3.7 shows the performance characteristics of the high-pass filter. Note that this filter also has purely linear phase response.

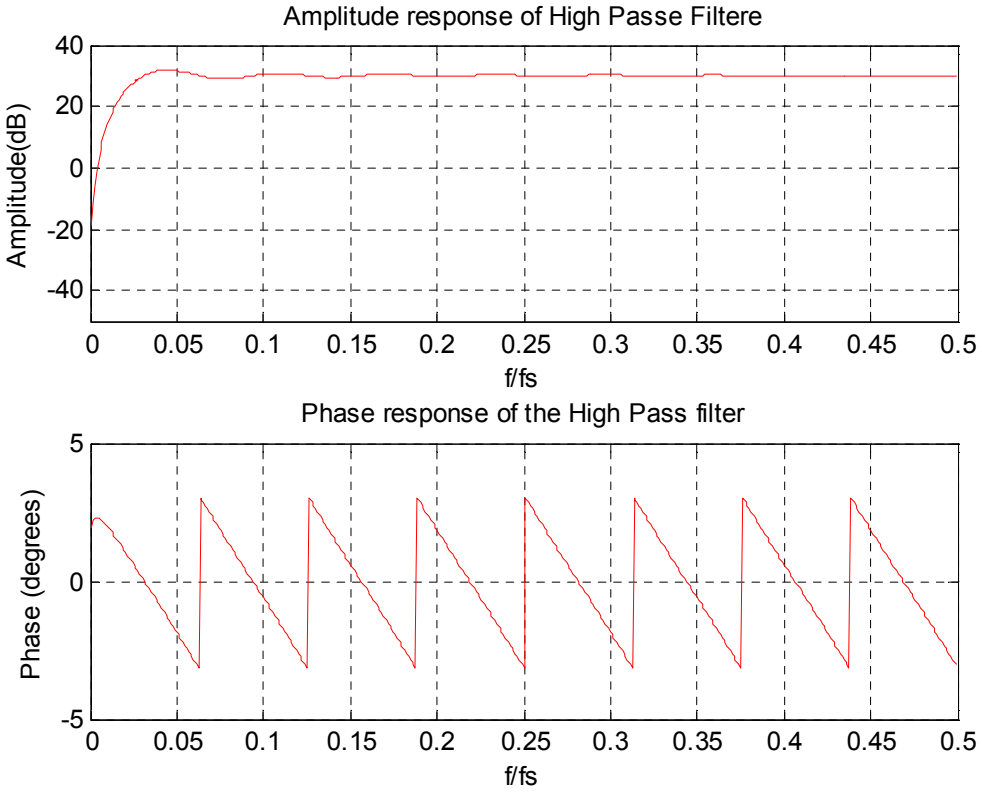

Figure 3.7 Amplitude response; Phase response of the High pass filte*r.*

III.4.3 Derivative filter

After the signal has been filtered, it is then differentiated to provide information about the slope of the QRS complex. A five-point derivative has the transfer function:

$$H(Z) = 0.1(2 + Z^{-1} - Z^{-3} - 2\ Z^{-4}) \qquad (3.15)$$

The difference equation of this derivative filter is:

$$y(nT) = (2x(nT) + x(nT - T) - x(nT - 3T) - 2x(nT - 4T)/8 \qquad (3.16)$$

The fraction 1/8 is an approximation of the actual gain of 0.1. This derivative approximates the ideal derivative in the dc through 30 Hz frequency range. The derivative has a filter delay of two samples (or 10 ms).

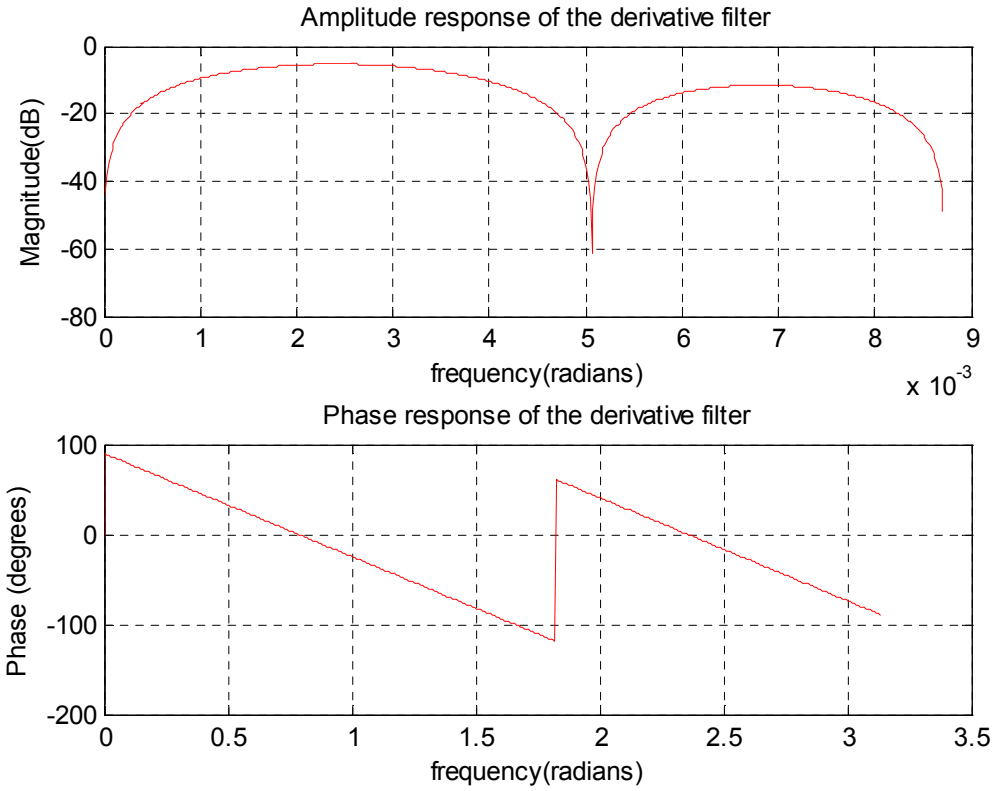

Figure 3.8 Amplitude response; Phase response of the derivative filter.

Note that the amplitude response approximates that of a true derivative up to about 20Hz. This is the important frequency range since all higher frequencies are significantly attenuated by the bandpass filter.

III.4.4 Squaring function

After differentiation step is the squaring function that the signal now passes through witch is a nonlinear operation. The equation of this operation is:

$$y(nT) = [x(nT)]^2 \qquad (3.17)$$

This operation makes all data points in the processed signal positive, and it amplifies the output of the derivative process nonlinearly. It emphasizes the higher frequencies in the signal, which are mainly due to the QRS complex.

III.4.5 Moving window integration

The slope of the R wave alone is a necessary condition but is insufficient way to detect the QRS complexes, because there are many abnormal QRS complexes that have large amplitudes and long durations might not be detected using only the information about slope of the R wave . Thus, we need to extract more information from the signal to detect a QRS event.

Moving window integration extracts features in addition to the slope of the R wave. It is implemented with the following difference equation:

$$y(nT) = (1/N)[x(nT - (N - 1)T) + x(nT - (N - 2)T) + \cdots + x(nT)] \qquad (3.18)$$

Where *N* is the number of samples in the width of the moving window, the value of this parameter should be chosen carefully. Figure 3.9 illustrates the relationship between the QRS complex and the window width. The width of the window should be approximately the same as the widest possible QRS complex. If the size of the window is too large, the integration waveform will merge the QRS and T complexes together. On the other hand, if the size of the window is too small, a QRS complex could produce several peaks at the output of the stage. The width of the window should be chosen experimentally. For a sample rate of 200 Hz, the window chosen for this algorithm was 30 samples wide (which correspond to 150 ms).

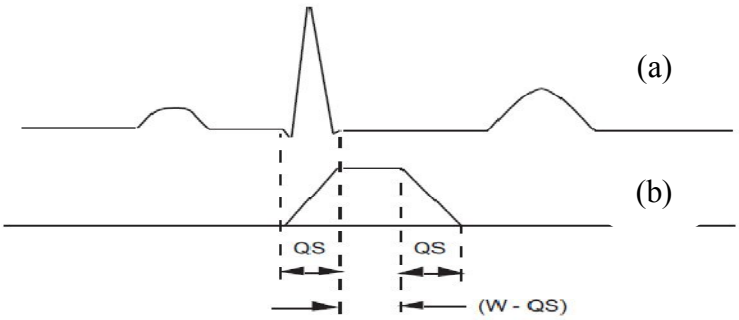

Figure 3.9 The relationship of a QRS complex to the moving integration waveform. (a) ECG signal. (b) Output of moving window integrator. QS: QRS width. W: width of the integrator window.

- After applied this filtrate stage the next step is the decision stage witch based the adaptive thresholds.

III.4.6 QRS detection using Adaptive thresholds

In this stage of the QRS detection algorithm Pan and Tompkins used an upward and downward thresholds to identify that the signal peaks are defined as those of the QRS complexes (R peak) while noise peaks are those of T waves.

Two set of thresholds are used (the waveform from the moving window integrator and the bandpass filter), each of which has two thresholds levels. The set of thresholds that is applied to the waveform from the moving window integrator is:

$SPKI = 0.125\ PEAKI + 0.875\ SPKI$ if *PEAKI* is the signal peak

$NPKI = 0.125\ PEAKI + 0.875\ NPKI$ if *PEAKI* is the noise peak

$$THRESHOLD\ I1 = NPKI + 0.25\ (SPKI - NPKI)$$

$$THRESHOLD\ I2 = 0.5\ THRESHOLD\ I1$$

All the variables in these equations refer to the signal of the integration waveform and are described below:

PEAKI is the overall peak.

SPKI is the running estimate of the signal peak.

NPKI is the running estimate of the noise peak.

THRESHOLD I1 is the first threshold applied.

THRESHOLD I2 is the second threshold applied.

When the signal changes direction within a certain time interval in this case a peak is determined. The signal peak *SPKI* is the peak that the algorithm has learned to be that of the QRS complex. While *NPKI* peak is any peak that is not related to the QRS complex. As can be seen from the equations, new values of thresholds are calculated from previous ones, and thus the algorithm adapts to changes in the ECG signal from a particular person. From the equations you can remark that new values of thresholds are calculated from previous ones, and thus the algorithm adapts to changes in the ECG signal from a particular person.

Whenever a new peak is detected, it must be categorized as a noise peak or a signal peak. If the peak level exceeds *THRESHOLD I1* during the first analysis of the signal, then it is a QRS peak. If searchback technique (explained in the next section) is used, then the signal peak should

exceed *THRESHOLD I2* to be classified as a QRS peak. If the QRS complex is found using this second threshold level, then the peak value adjustment is twice as fast as usual:

$$SPKI = 0.25\ PEAKI + 0.75\ SPKI$$

The set of thresholds that is applied to the waveform from the bandpass filter is:

$SPKF = 0.125\ PEAKF + 0.875\ SPKF$ if *PEAKF* is the signal peak

$NPKF = 0.125\ PEAKF + 0.875\ NPKF$ if *PEAKF* is the noise peak

$$THRESHOLD\ F1 = NPKF + 0.25\ (SPKF - NPKF)$$

$$THRESHOLD\ F2 = 0.5\ THRESHOLD\ F1$$

All the variables in these equations refer to the signal of the bandpass filter waveform and are described below:

PEAKIF is the overall peak.

SPKI F is the running estimate of the signal peak.

NPKF is the running estimate of the noise peak.

THRESHOLD F1 is the first threshold applied.

THRESHOLD F2 is the second threshold applied.

When the QRS complex is found using the second threshold:

$$SPKF = 0.25\ PEAKF + 0.75\ SPKF$$

A peak must be recognized as such a complex in both the integration and bandpass filtered waveforms to be identified as QRS complex.

For irregular heart rates, the first threshold of each set is reduced by half so as to increase the detection sensitivity and to avoid missing beats:

$$THRESHOLD\ I1 = 0.5\ THRESHOLD\ I1$$

$$THRESHOLD\ F1 = 0.5\ THRESHOLD\ F1$$

III.4.7 Searchback technique

In order to implement the searchback technique, the algorithm of Pan and Tompkins maintains two RR interval averages. The first average, *RR AVERAGE1*, is that of the eight most recent heartbeats. The other average, *RR AVERAGE2*, is the average of the eight most recent beats which had RR intervals that fell within a certain range.

$$RR\ AVERAGE1 = 0.125\ (RRn-7 + RRn-6 + \ldots + RRn) \quad (3.19)$$

$$RR\ AVERAGE2 = 0.125\ (RR'n-7 + RR'n-6 + \ldots + RR'n) \quad (3.20)$$

The *RR'n* values are the RR intervals that fell within the following limits:

$$RR\ LOW\ LIMIT\ =\ 92\%\ \times\ RR\ AVERAGE2 \quad (3.21)$$

$$RR\ HIGH\ LIMIT\ =\ 116\%\ \times\ RR\ AVERAGE2 \quad (3.22)$$

Whenever the QRS waveform is not detected for a certain interval, *RR MISSED LIMIT*, then the QRS is the peak between the established thresholds mentioned in the previous section that are applied during searchback.

$$RR\ MISSED\ LIMIT\ =\ 166\ \%\ \times\ RR\ AVERAGE2 \quad (3.23)$$

The heart rate is said to be normal if each of the eight most recent RR intervals are between the limits established by *RR LOW LIMIT* and *RR HIGH LIMIT*.

$$RR\ AVERAGE2\ \ \leftarrow\ RR\ AVERAGE1 \quad (3.24)$$

When an RR interval is less than 360ms a judgement is made to determine whether the current QRS complex has been correctly identified or whether it is really a T wave. If the maximal slope that occurs during this waveform is less than half of the QRS waveform that proceeded, it is identified to be a T wave; otherwise, it is called a QRS complex.

Conclusion

The study of each part/block of the Pan and Tompkins algorithm allowed us to well to extract the characteristics and understand the goal of each block in the process of the QRS complex detection in the ECG signals. In order to push farther acknowledges acquired in this chapter. For this reason we will try in the next chapter to implement them to handle a real world problem (e.g. ECG signals) and to access the expected performance

Chapter IV

Results and Discussion

Introduction

Because the QRS complex is the major feature in ECG signal, we applied Pan and Tompkins algorithm. In order to implement it, we use the same parameter described in the paper [20] which are explained in the previous chapter. We use the MATLAB program to test result of the algorithm.

IV.1 Presentation of the database

Several standard ECG database are available for the evaluation of the software QRS detection algorithm. In our case we used the MIT/BIH arrhythmia database. This physiological database provided by the collaboration between Massachusetts Institute of Technology and Boston's Beth Israel Hospital. It has been achieved between 1975 and 1979 and it distributed in 1980 [33].

The MIT/BIH arrhythmia database contains 48 half hour of two channel ambulatory ECG recording, obtained from 47 subjects studied by the BIH arrhythmia laboratory .The subjects were 25 men aged between 32 and 89 years and 22 women aged between 23 and 89 years. Twenty -three records (numbered from 100 to 124 inclusive with some numbers missing) were selected randomly form a set of 4000 24-hour ambulatory ECG recording collected from a mixed population of inpatients (about 60%) and outpatients (about 40%) at Boston's Beth Israel hospital, the remaining 25 recordings (numbered from 200 to 234 inclusive, again with some numbers missing) were selected from the same set to include less common but clinically significant arrhythmias that would not be well-represented in a small random sample. Records in the second group were chosen to include complex ventricular, junctional, and supraventricular arrhythmias and conduction abnormalities. Several of these records were selected because features of the rhythm, QRS morphology variation, or signal quality may be expected to present significant difficulty to arrhythmia detectors; these records have gained considerable notoriety among database users.

The recordings were digitized at 360 samples per second per channel with 11 bit resolution. Two or more cardiologists independently annotated each record. These valuable resources can be downloaded from the free-access website (physionet.org) [33].

IV.2 Files in the MIT/BIH database

For each record of the database contains three different files with the following extensions: .dat, .hea and .atr.

IV.2.1 The data file (*.dat)

Almost all records include a binary file containing digitized samples of the ECG signal. Two different signals corresponding to the two leads are stored in the same file, e.g. 100.dat, these file can be very large.

IV.2.2 The header file (*.hea)

Is a short text file that describes the signals .It contains the parameters of interpretation of the data files and allows the program to use (the name of the signal, storage format, sampling frequency, record duration and starting time ....etc).

IV.2.3 The annotation file (*.atr)

It includes position or times of occurrence of the QRS complex (heart beat), and a set of label given the order of the R peak and type of the QRS complex (normal or abnormal). These locations were manually marked by several cardiologists.

IV.3 Power spectrum of the ECG

The ECG waveform contains, in addition to the QRS complex, P and T waves, 60 Hz noise from powerline interference, EMG from muscles, motion artefact from the electrodes and skin interface, and possibly other interference from electrodes surgery equipment in the operating room. Many clinical instruments such as a cardiotachometer and an arrhythmia monitor require accurate real-time QRS detection. It is necessary to extract the signal of interest, the QRS complex, from the other noise sources such as the P and T waves. Figure 1.4 summarizes the relative power spectra of the ECG, QRS complexes, P and T waves, motion artefact, and muscle noise based on their previous research [31].

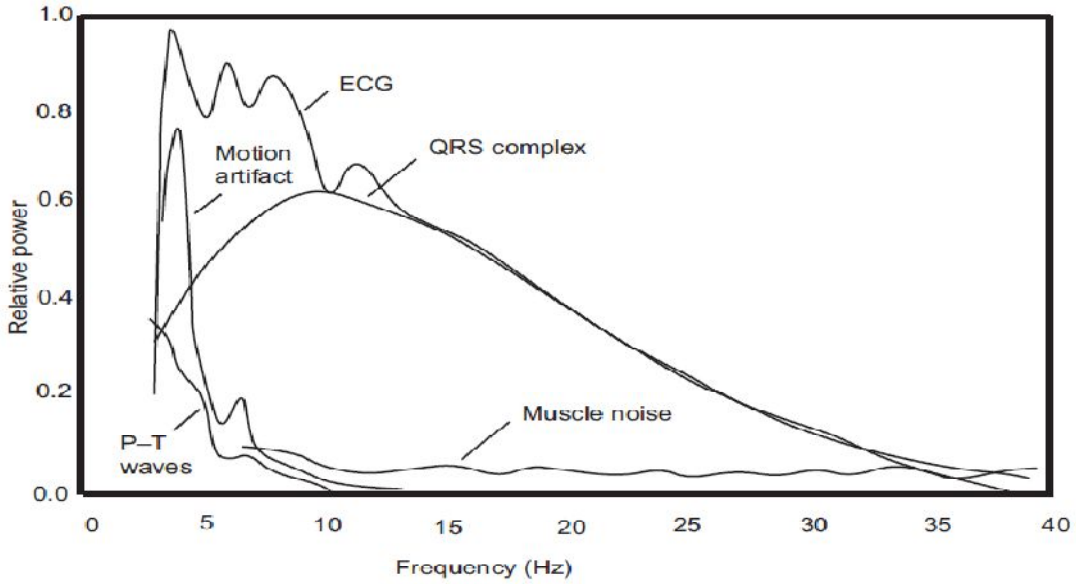

Figure 4.1 Relative power spectrum of QRS complex, P and T waves, muscle noise and motion artifacts.

For this reason Pan and Tompkins used a set of filters to reduce the noise in the ECG signal in order to facility the detection of the QRS complex. The influence of this filters and the results obtained are explaining in the next section.

IV.4 QRS Detection Algorithm

The scheme of QRS detection (actually R peak detection) algorithm is sketched in Figure 4.

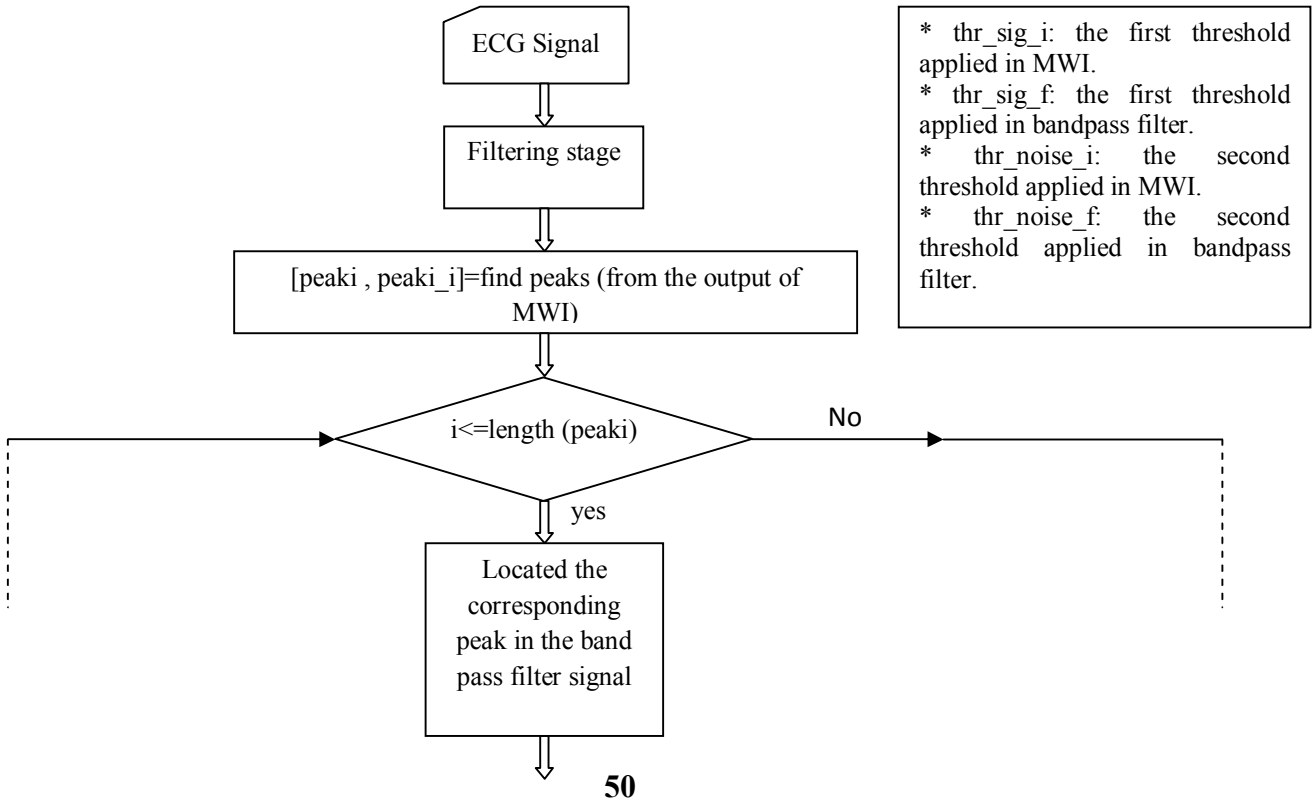

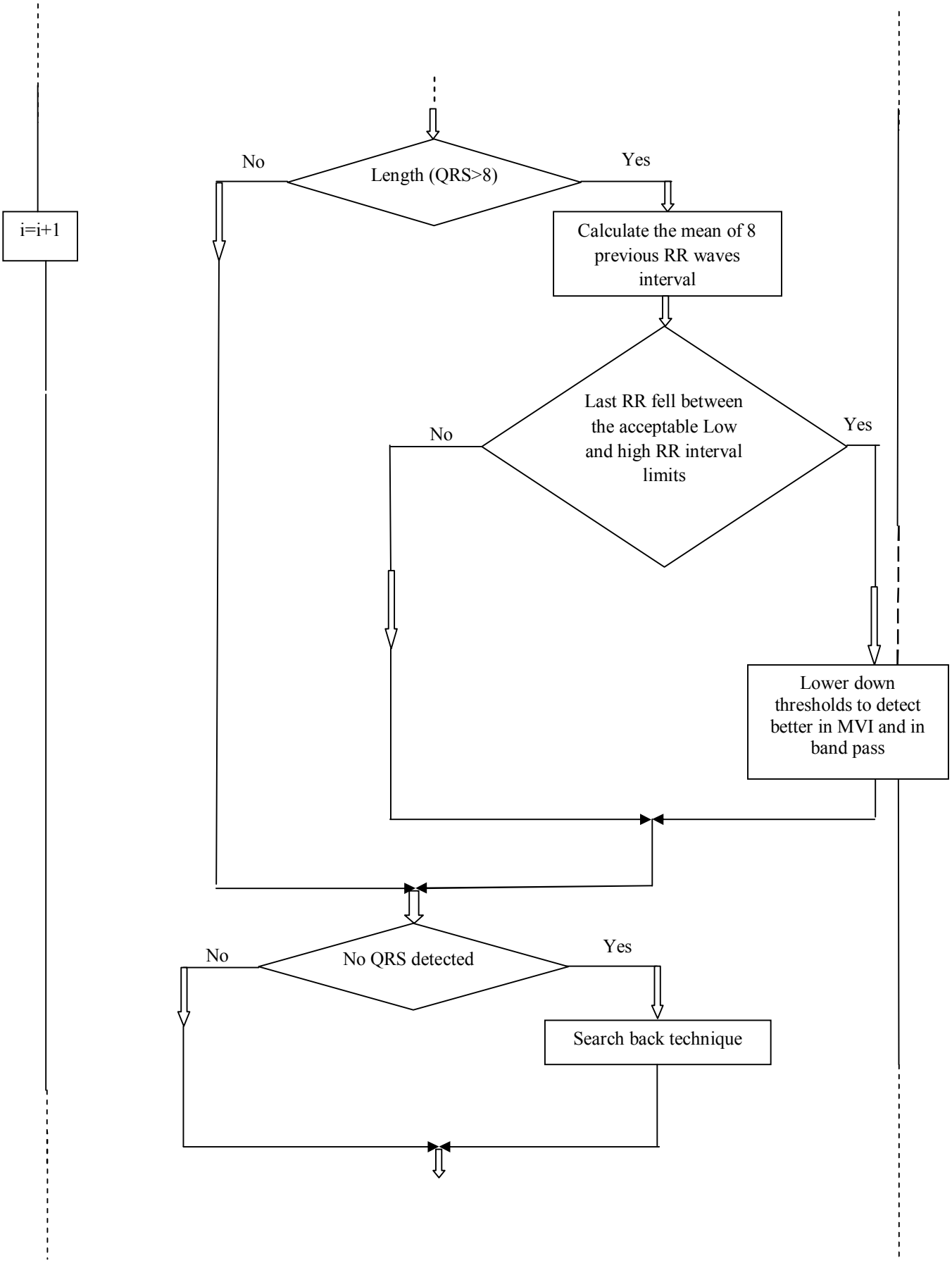
i=i+1
No
Length (QRS>8)
Yes
Calculate the mean of 8 previous RR waves interval
Last RR fell between the acceptable Low and high RR interval limits
No
Yes
Lower down thresholds to detect better in MVI and in band pass
No
No QRS detected
Yes
Search back technique

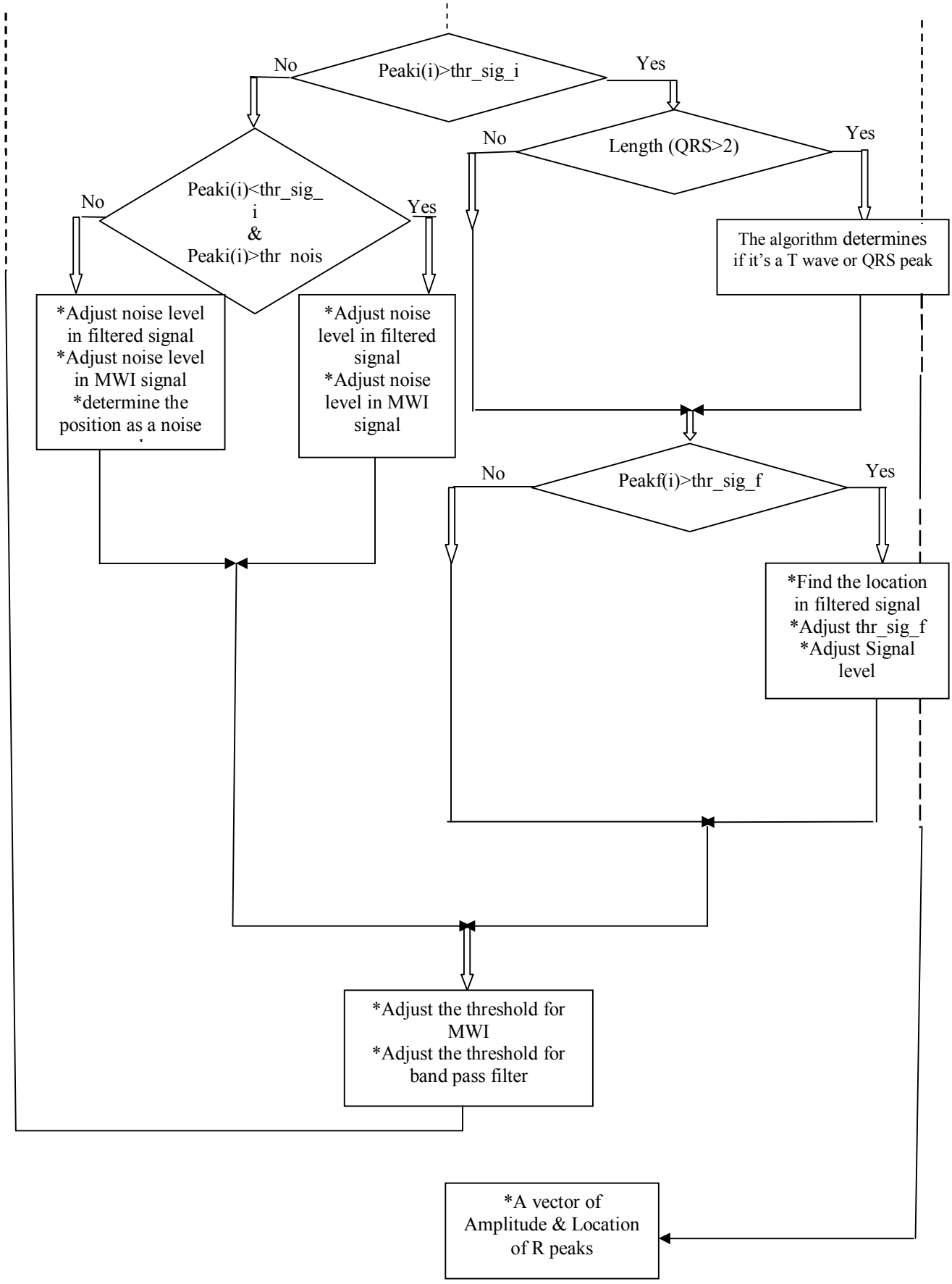

Figure 4.2 The QRS Detection Procedure.

IV.5 Results obtained by the implementation of Pan and Tompkins filter blocks

To test the filter stage of the algorithm, we use a sampled ECG possessed from the MIT/BIH data base (the record 100) because is the simple and the easy signal in the database. We chose the first five second of the record. This is shown in Figure 4.2, where you can notice that the signal suffer of the baseline drift and noises which are the main problem in process of QRS detection.

IV.5 .1 The bandpass filter

As described in the previous chapter, that the bandpass filter implemented in Pan and Tompkins algorithm is composed of cascade low pass and high pass filter. In the next paragraph we show the result of the output of each one.

IV.5.1.1 The low pass filter

As mentioned in (chapter III), that the low pass filter implemented in the algorithm has a characteristic to attenuate all the higher frequencies. The Figure 4.3 shows the ECG signal of Figure 4.2 after processing with the low-pass filter. The most noticeable result is the attenuation of the higher frequency QRS complex. Any 60-Hz noise or muscle noise present would have also been significantly attenuated.

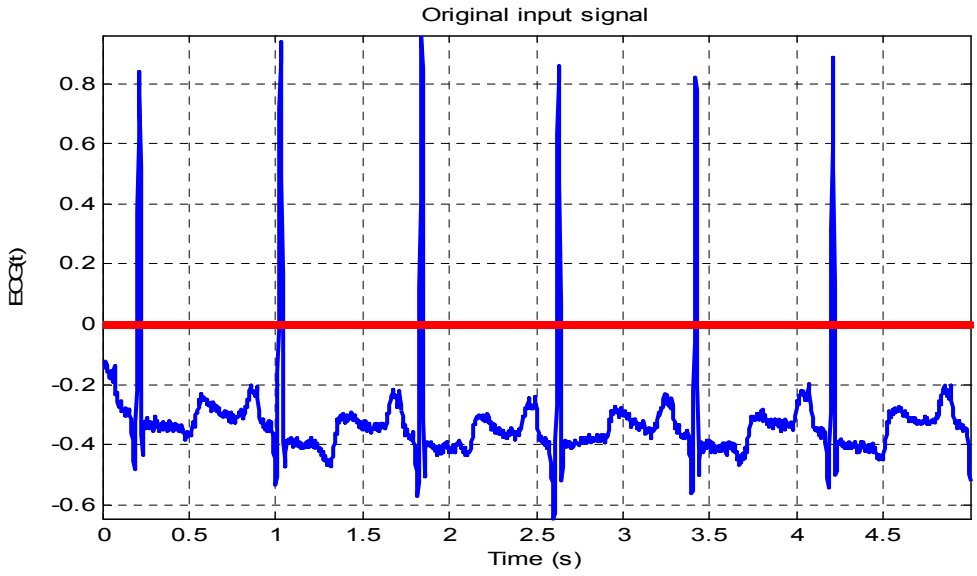

Figure 4.3 Original input ECG signals 100.dat

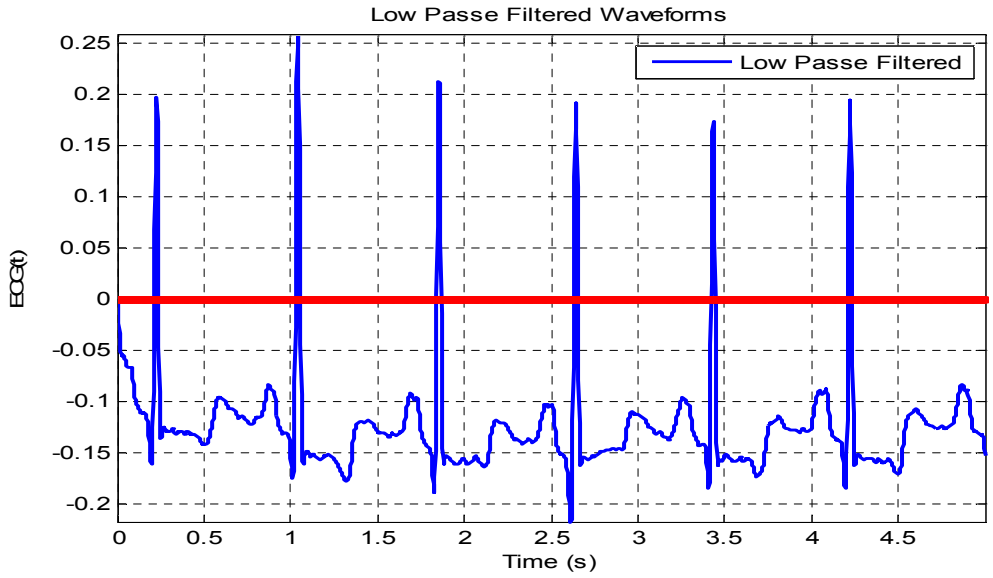

Figure 4.4 Low-pass filtered ECG signal.

IV.5.1.2 The high-pass filter

The implementation of the High-pass filter and its performance characteristics are described in the previous chapter. The Figure 4.4 shows the ECG signal of Figure 4.3 after processing with the high-pass filter (the out-put of the band pass filter). We can notice that after filtering the signal by the band pass filter the baseline drift was eliminate from the ECG signal.

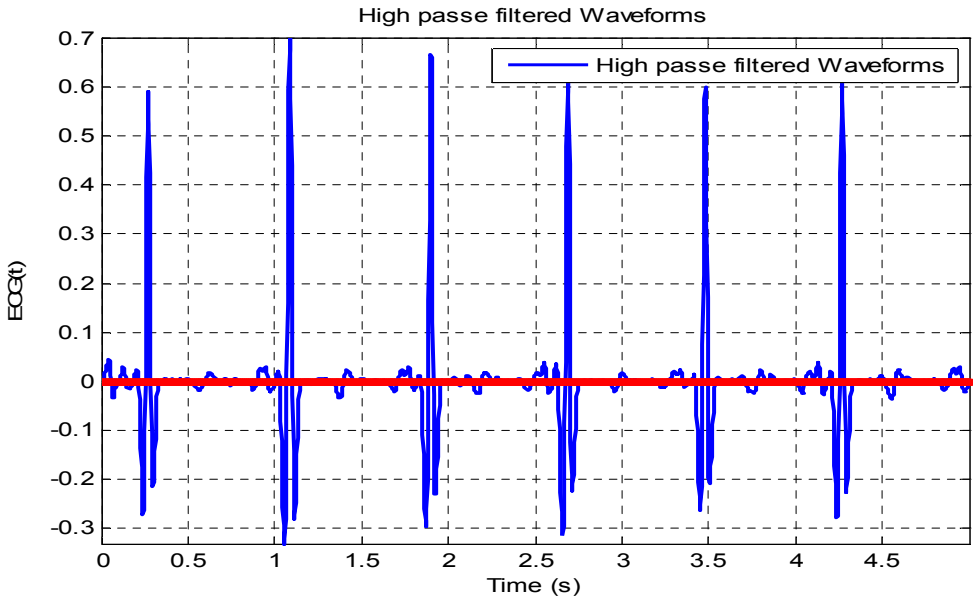

Figure 4.5 High-pass filtered ECG signal.

IV.5.2 Derivative filter

After the signal has been feed to the band-pass filter, the result is then differentiated to provide information about the slope of the QRS complex. The transfer function and the characteristics of the filter are described in chapter III. The Figure 4.5 shows the resultant signal after passing through the cascade of filters (band-pass filter) including the differentiator. We can observe in the graph that P and T waves are further attenuated while the peak-to-peak signals corresponding to the QRS complex are amplified.

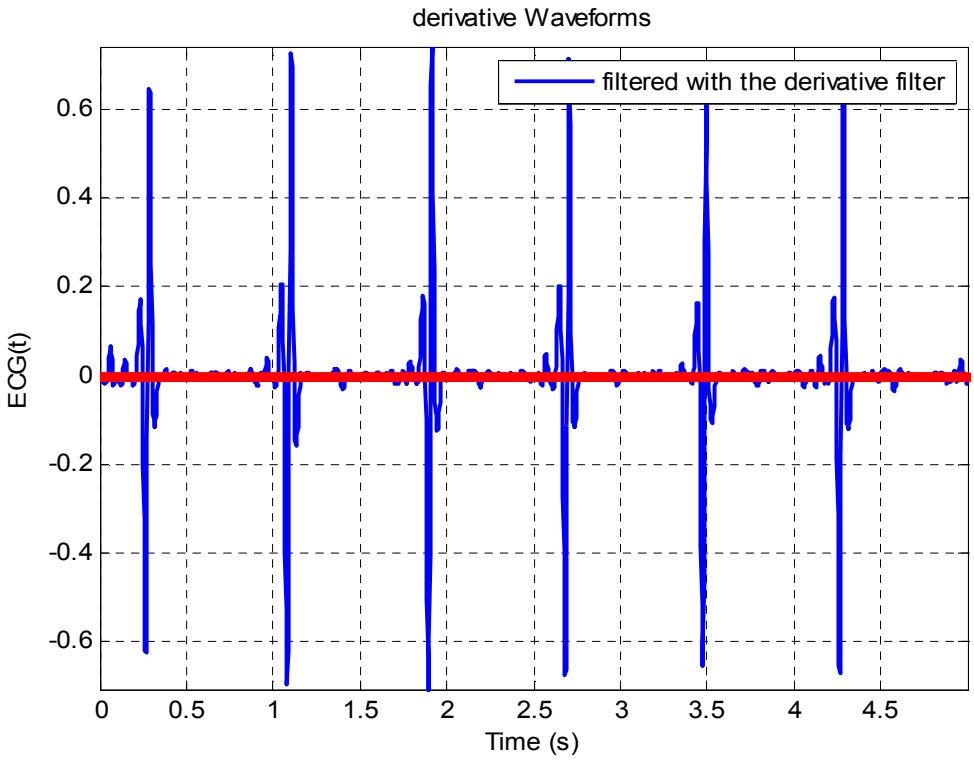

Figure 4.6 ECG signal after bandpass filtering and differentiation

IV.5.3 Squaring function

The signal obtained from the derivative step passes through is a nonlinear operation (squaring function). This operation makes all data points by points in the processed signal positive, and it amplifies the output of the derivative process nonlinearly. Figure 4.6 shows the results of this processing step.

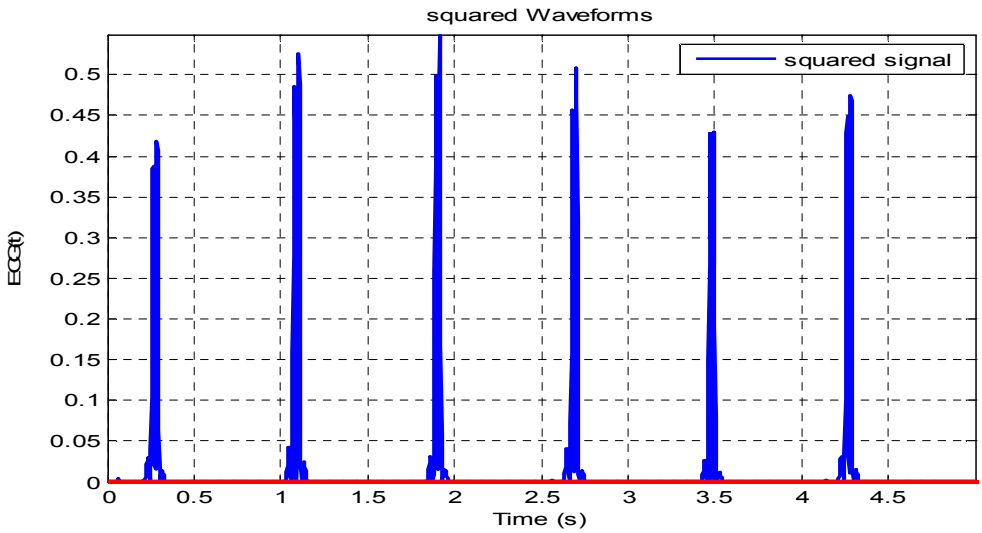

Figure 4.7 ECG signal after squaring function.

IV.5.4 Moving window integral

After squaring process which makes all data of the signal positive, the next step is to smooth the signal obtained by moving window integration (MWI) technique. It extracts features in addition to the slope of the R wave from the signal to detect a QRS event. The size of the window (numbers of samples) should be chosen carefully, because it should be approximately the same as the widest possible QRS complex. We know that the QRS complex hasn't the same width; it changes the state according to the person. In our case we chose the size of moving window integration equal to 54 samples (which corresponds to 150 ms, because the sampling frequency of the signal equal to 360 Hz). Figure 4.7 shows the output of this processing step.

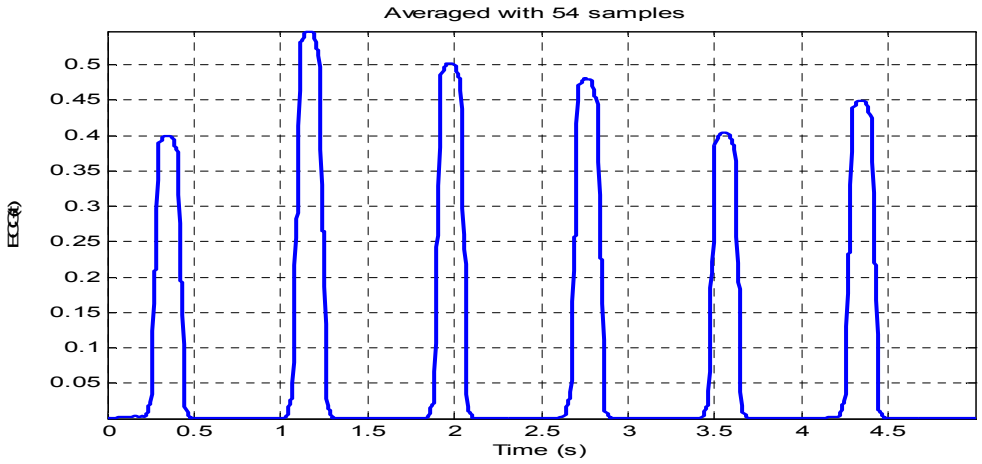

Figure 4.8 Signal after moving window integration.

The next step in the algorithm is the most important phase. The goal of this phase is to detect the R peaks accurately based on adaptive thresholds and search back technique, which are described in more details in the next section.

IV.6 Decision Rules

At this point in the algorithm, the preceding stages have produced a roughly pulse-shaped waveform at the output of the moving window integration (MWI). The determination as to whether this pulse corresponds to a QRS complex (as opposed to a high-sloped T-wave or a noise artefact) is performed with an adaptive thresholding operation and other decision rules outlined below.

IV.6.1 Fiducial mark (Find Peaks)

The waveform is first processed to produce a set of weighted unit samples at the location of the moving window integration (MWI) maxima. This is done in order to localize the QRS complex to a single instant of time. The w[k] weighting is the maxima value. We not that a minimum distance of 72 samples is considered between each R wave since in physiological point of view no RR wave can occur in less than 200 msec distance. This limit allowed this parameter (find peaks) free and it has a major influence on the detection of QRS complex.

IV.6.2 Thresholding

When analyzing the amplitude of the moving window integration (MWI) output, the algorithm uses two threshold values (*THRESHOLD I1* and *THRESHOLD I2* appropriately initialized during a brief 2 second training phase [18].)

- *THRESHOLD I1*= 0.25 of the max amplitude of MWI
- *THRESHOLD I2*== 0.5 of the mean amplitude MWI

That continuously adapt to changing ECG signal quality. The first step uses these thresholds to classify the each non-zero sample current peak (PEAKI) as either signal or noise:

If *PEAKI* > *THRESHOLD I1,* that location is identified as a QRS complex candidate and the signal level (SPKI) is updated:

SPKI = 0.125 *PEAKI* + 0.875 *SPKI*.

If *THRESHOLD I2* < *PEAKI* < *THRESHOLD I1*, then that location is identified as a noise peak and the noise level (*NPKI*) is updated:

NPKI = 0.125 *PEAKI* + 0.875 *NPKI*

Based on new estimates of the signal and noise levels (SPKI and NPKI, respectively) at that point in the ECG, the thresholds are adjusted as follows:

THRESHOLD I1= NPKI + 0.25 (*SPKI- NPKI*)

THRESHOLD I2= 0.5 (*THRESHOLD I1*)

These adjustments lower the threshold gradually in signal segments that are deemed to be of poorer quality. The same procedure is applied to the output of the band pass filter, after found the position of the QRS complexes corresponding to moving window integration (MWI).

IV.6.3 Searchback for missed QRS complexes

In the thresholding step above, if *PEAKI* < *THRESHOLD I1*, the peak is deemed not to have resulted from a QRS complex. If however, an unreasonably long period has expired without an above threshold peak, the algorithm will assume a QRS has been missed and perform a searchback. This limits the number of false negatives. The minimum time used to trigger a searchback is 1.66 times the current R peak to R peak time period (called the RR interval) [18], this value has a physiological origin, the time value between adjacent heartbeats cannot change more quickly than this. The missed QRS complex is assumed to occur at the location of the highest peak in the interval that lies between *THRESHOLD I1* and *THRESHOLD I2*. In this algorithm, two average RR intervals are stored, the first RR interval is calculated as an average of the last eight QRS locations in order to adapt to changing heart rate and the second RR interval mean is the mean of the most regular RR intervals. The threshold is lowered if the heart rate is not regular to improve detection.

IV.6.4 Elimination of multiple detections

It is impossible for a legitimate QRS complex to occur if it lies within 200 ms after a previously detected one. This constraint is a physiological during which ventricular depolarization cannot occur despite a stimulus [18]. As QRS complex candidates are generated, the algorithm eliminates such physically impossible events, thereby reducing false positives.

IV.6.5 T wave discrimination

Finally, if a QRS candidate occurs after the 200ms refractory period but within 360ms of the previous QRS, the algorithm determines whether this is a genuine QRS complex of the next heartbeat or an abnormally prominent T wave. This decision is based on the mean slope of the waveform at that position. A slope of less than one half that of the previous QRS complex is consistent with the slower changing behaviour of a T wave otherwise, it becomes QRS complex.

IV.6.6 The final stage

The output of R waves detected in the smoothed signal is analyzed and double checked with the help of the output of the bandpass signal to improve the detection and find the original index of the real R waves on the raw ECG signal.

The results of the implemented algorithm of Pan and Tompkins using MATLAB are shown in the following table:

records	Peaks in the MIT/BIH	Peaks detected with our Implemented Algorithm	Peaks detected with Pan and Tompkins Algorithm	Failed detection with our Implemented Algorithm	Failed detection with Pan and Tomkins Algorithm
100	2273	2273	2273	0	0
101	1865	1866	1870	1	5
102	2187	2187	2187	0	0
103	2084	2083	2084	-1	0
104	2229	2230	2231	1	2
105	2572	2578	2639	6	67
106	2027	2002	2032	-25	5
107	2137	2126	2137	-11	0
108	1763	1767	1962	4	199
109	2532	2527	2532	-5	0
111	2124	2123	2125	-1	1
112	2539	2540	2539	1	0
114	1879	1872	1882	-7	3
115	1953	1953	1935	0	0
116	2412	2392	2415	-20	-19
117	1535	1535	1536	0	1
118	2278	2278	2276	0	-2
119	1987	1988	1988	1	1
121	1863	1863	1867	0	4
122	2476	2476	2477	0	1
123	1518	1515	1518	-3	0
124	1619	1611	1619	-8	0
200	2601	2603	2607	2	6
201	1963	1910	1963	-53	0
202	2136	2130	2136	-6	0
203	2980	2903	3035	-77	55
205	2656	2648	2656	-8	0
207	1860	2079	1866	219	6
208	2955	2838	2960	-117	5
209	3005	3005	3007	0	2

210	2650	2600	2649	-50	-1
212	2748	2748	2748	0	0
213	3251	3244	3252	-7	1
214	2262	2255	2264	-7	2
215	3363	3347	3363	-16	0
217	2208	2203	2212	-5	4
219	2154	2151	2154	-3	0
220	2048	2048	2048	0	0
221	2427	2421	2429	-6	2
222	2483	2484	2585	1	102
223	2605	2596	2606	-9	1
228	2053	2058	2078	5	25
230	2256	2256	2257	0	1
231	1571	1571	1886	0	315
232	1780	1786	1786	6	6
233	3079	3065	3079	-14	0
234	2753	2750	2753	-3	0

Table 4.1 Results obtained in term of detection

From the table we can see that there are 7 cases in which our implementation algorithm gives the same results as Pan and Tompkins. Also, we see that there are 40 cases in which the results are different from those published in Pan and Tompkins paper [20], from those 40 records there is 25 cases which are worst and 15 cases which are better than Pan and Tomkins [20]. In contrast to Pan and Tompkins algorithm, we can see that our implementation has a less failed detection peaks, 709 versus 844 for the published results in [20].

Concerning the better cases, we can see from the following histogram that our implemented algorithm is much better than those of Pan and Tompkins results the obtained result in terms of R detection. We believe that the obtained improvement in our case is due to the best choice of the parameters (MWI= 54 samples and FP=72samples).

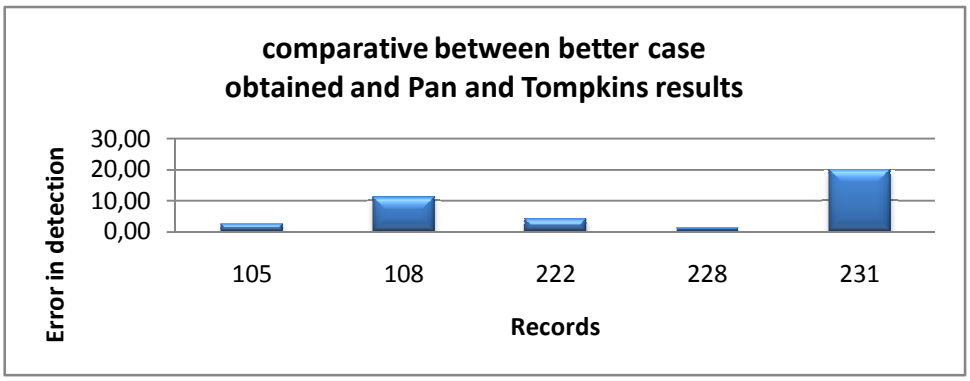

Figure 4.9 Comparative of some between the better cases obtained and Pan and Tompkins results.

For the worst cases, to explain the difference in term of detection between our implemented and the one described in Pan and Tompkins paper, we will try to tune some of the free parameters separately; in this case we choose MWI and FP only, to show their impact on the obtained results.

IV.7 The influence of the width of the moving window integrator (MWI)

In this section we setup up an experiment to show the influence of the length of the moving window integrator (MWI) on the detection process. In other terms, how many samples we have to use as a length of the MWI to obtain a better QRS complex selection in each record. The experiment consists to fix the FP parameter to 72 samples and iteratively change the value of MWI in the interval [38, 78] with step of 10 samples. The results obtained are shown in the following histograms.

The first example is the record 105 which contain 2572 beats in the MIT/BIH data base, the influence of the width of the moving window integrator in the detection is shown in the following histogram.

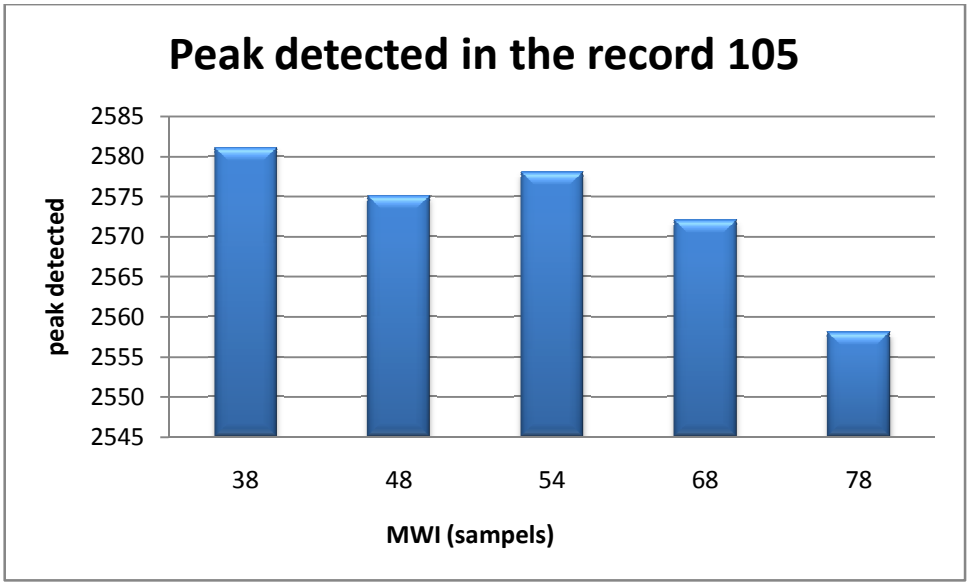

Figure 4.10 The variation of the peaks detected based on the length of MWI in the record 105.

We observe in the histogram the influence of the length of the MWI in the detection, the value of peak detected vary between 2558 and 2581 peaks. We obtain 2572 peaks which is the same number of beat in MIT/BIH data base with MWI=68 samples.

The flowing example is the record 108 which contain 1763 beats in the MIT/BIH data base, the influence of the width of the moving window integrator in the detection is shown in the following histogram.

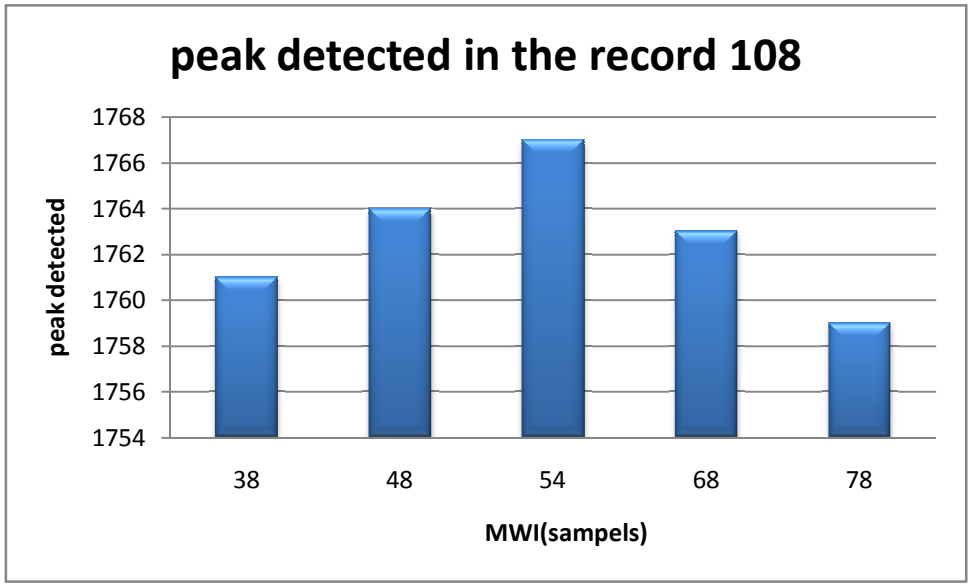

Figure 4.11 The variation of the peaks detected based on the length of MWI in the record 108.

We not from the histogram the influence of the length of the MWI in the detection, the value of peak detected vary between 1759 and 1767 peaks. We obtain 1763 peaks which is the same number of beat in MIT/BIH data base with MWI=68 samples.

On other example is the record 201 which contain 1963 beats in the MIT/BIH data base, the influence of the width of the moving window integrator in the detection is shown in the following histogram.

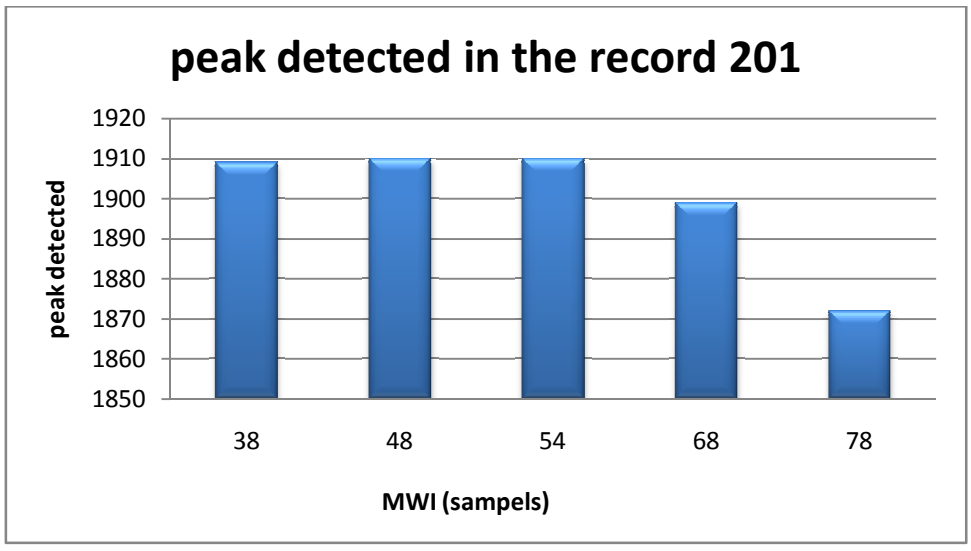

Figure 4.12 The variation of the peaks detected based on the length of MWI in the record 201.

We observe in the histogram the influence of the length of the MWI in the detection, the value of peak detected vary between 1872 and 1910 peaks. We obtain 1910 peaks which is the acceptable value with MWI=54 samples.

The last example is the record 202 which contain 2136 beats in the MIT/BIH data base, the influence of the width of the moving window integrator in the detection is shown in the following histogram.

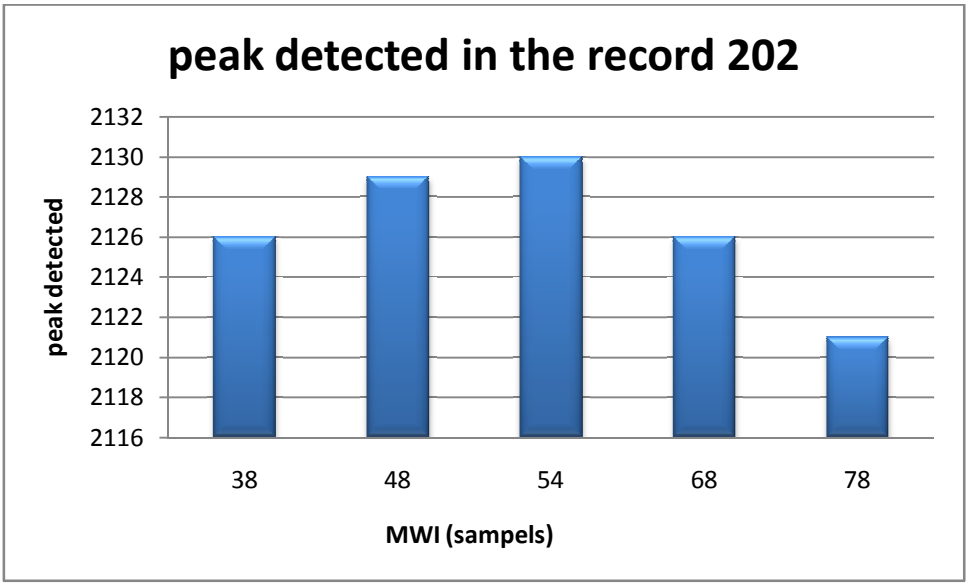

Figure 4.13 The variation of the peaks detected based on the length of MWI in the record 202.

We not from the histogram the influence of the length of the MWI in the detection, the value of peak detected vary between 2121 and 2130 peaks. We obtain 2130 peaks which is the acceptable value with MWI=54 samples.

From all this examples we conclude that the length of the MWI equal to 54 samples is the better value in term of detection.

IV.8 The influence Fiducial mark (find peaks)

In this section we setup up an experiment to show the influence of the parameter find peaks (FP) on the detection process, In other terms, how many samples we have to use as a distance between two peak for better QRS complex selection in each record. The experiment consists to fix the length of the moving window integrator MWI= 54 samples because this value corresponded to all the best numbers of detection, and iteratively change the value of FP in the interval [30, 90] with step of 10 samples. The results obtained are shown in the following histograms.

The first example is the record 108 which contain 1763 beats in the MIT/BIH data base, the influence of the number of samples in find peaks in the detection is shown in the following histogram.

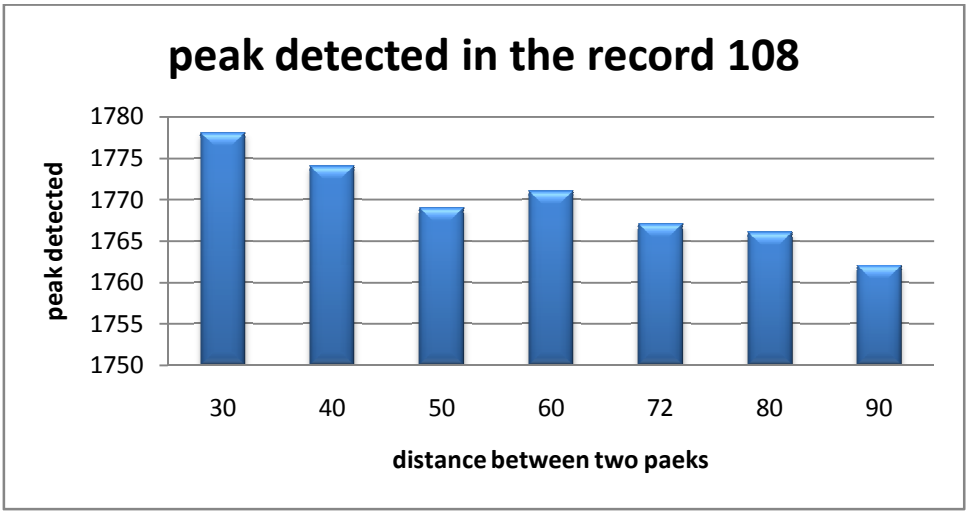

Figure 4.14 The variation of the peaks detected based on the min distance (FP) in the record 108.

The second example is the record 203 which contain 2980 beats in the MIT/BIH data base, the influence of the number of samples in find peaks in the detection is shown in the following histogram.

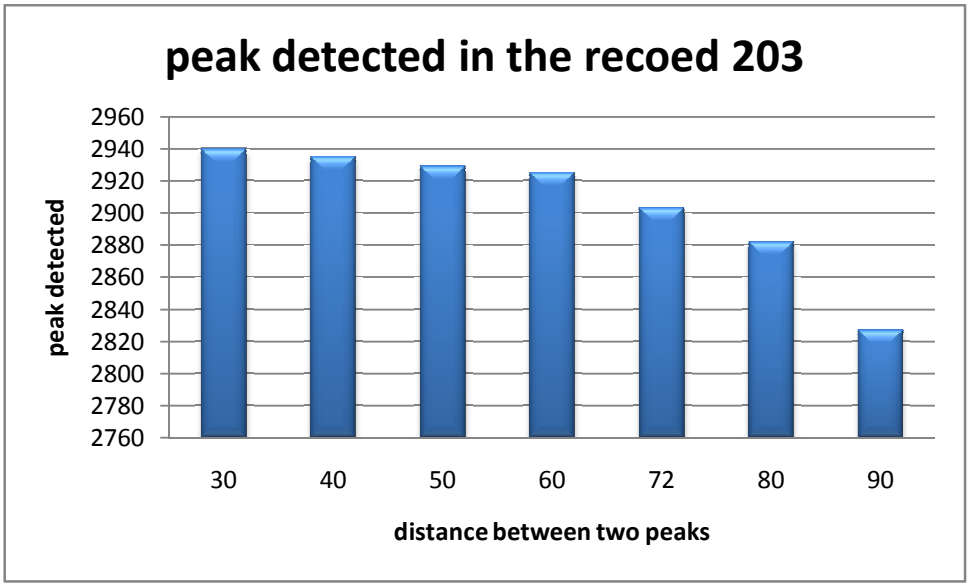

Figure 4.15 The variation of the peaks detected based on the min distance (FP) in the record 203.

The next example is the record 106 which contain 2027 beats in the MIT/BIH data base, the influence of the number of samples in find peaks in the detection is shown in the following histogram.

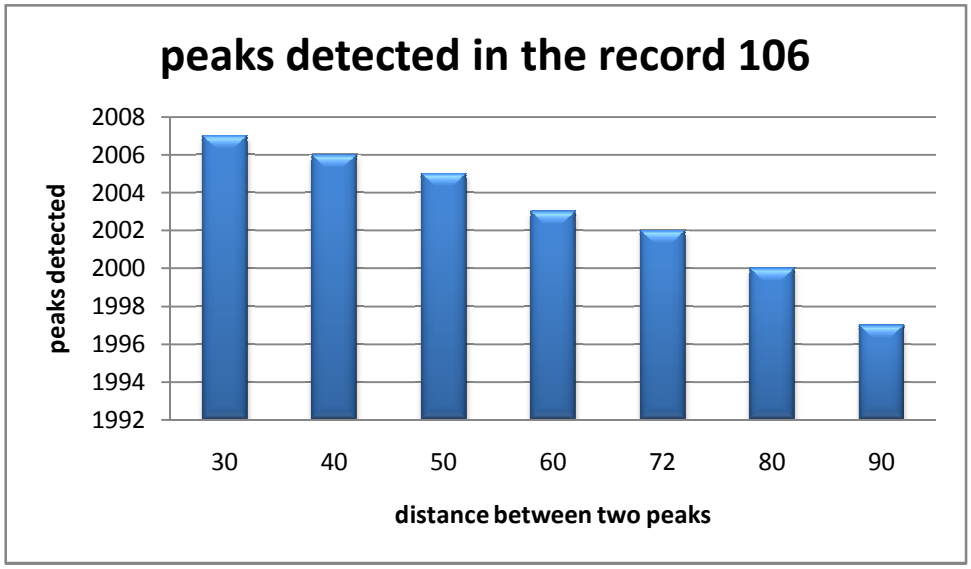

Figure 4.16 The variation of the peaks detected based on the min distance (FP) in the record 106

The last example is the record 207 which contain 1862 beats in the MIT/BIH data base, the influence of the number of samples in find peaks in the detection is shown in the following histogram.

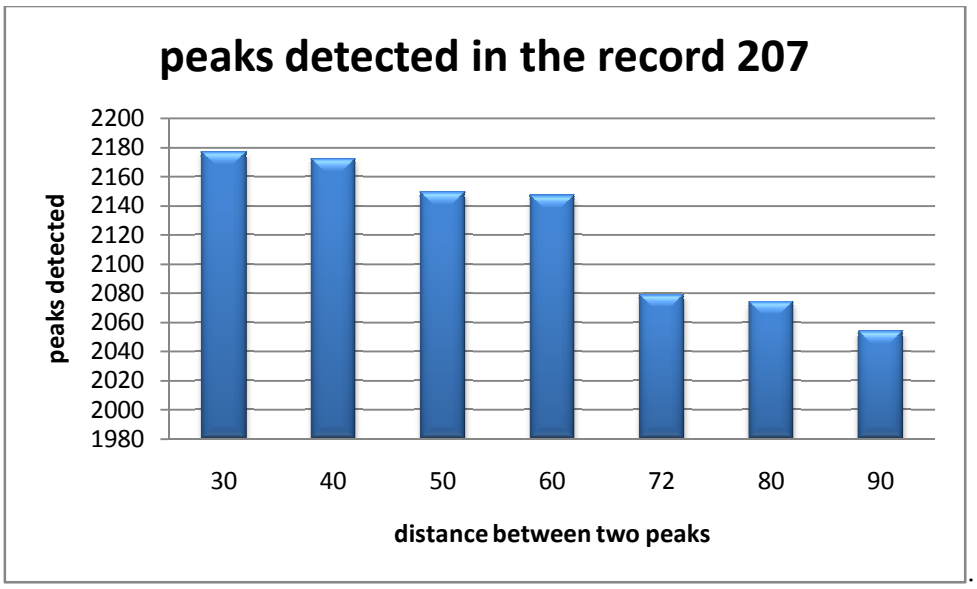

Figure 4.17 The variation of the peaks detected based on the min distance (FP) in the record 207.

From the previous figures we note that minimum distance between two peaks (value of PF) in the selection of QRS complex. FP has a major influence in the number of the peak detected,

the choice of the value of FP which mean the number of samples in our case equal to72 samples which is the good value in term of detection.

In order to assess the performance of the proposed algorithm we choose the well known MIT/BIH Arrhythmia database. The positive predictive is used for evaluating the ability of the algorithm to discriminate between true and false beats. Positive predictive (+*p*): It gives the percentage of heart beat detection which are true beats.

$$Positive\ predictive(\%) = \frac{TP}{TP+FP} \tag{4.1}$$

Where, *TP*=Number of true positive beat detected

FP= Number of false positive beat

Another important parameter that we have to take in consideration during the conduction of the experiment is the delay between the true (ATR file) and the detected QRS timing position. It's worth noting that in our case window of 72 samples around the detected beat is adopted in order to be able to evaluate the goodness of the detector in terms of detection of QRS complex. The figure below shows the delay between the peaks detected and the true annotation in the data base for the record 100.dat.

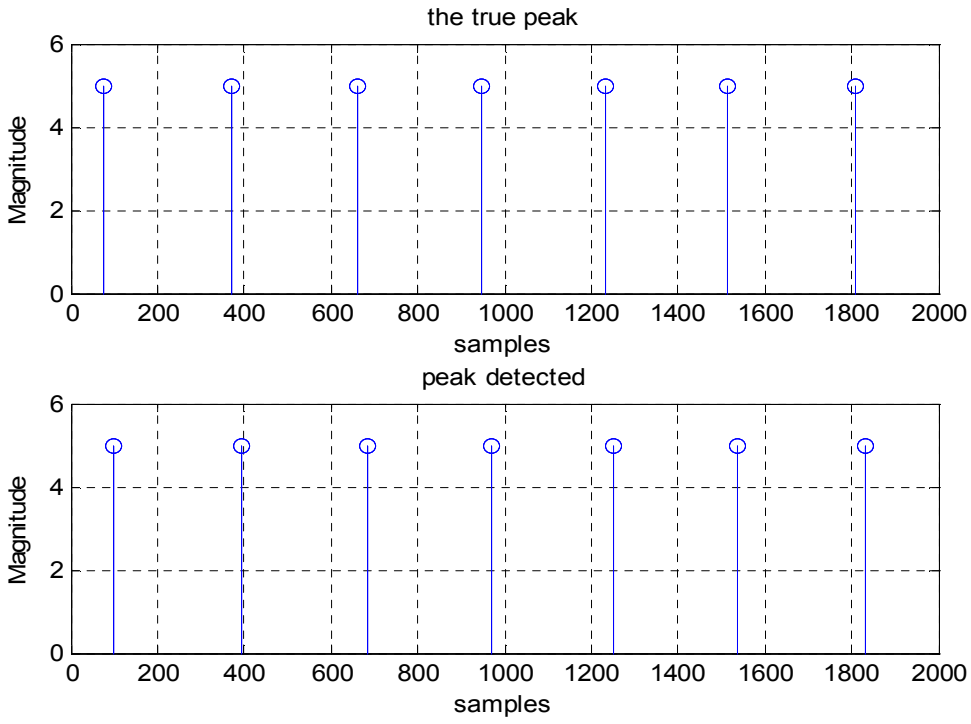

Figure 4.18 delay between the peak detected and the true annotation.

The following table shows the results obtained in the case in which we take the first 30s instead of the totality duration of the records:

Records	Totale beat	TP (Beats)	FP (Beats)	Positive Predictivity
100	37	37	0	100,00%
101	34	34	0	100,00%
102	36	36	0	100,00%
103	34	34	0	100,00%
104	37	37	0	100,00%
105	41	41	0	100,00%
106	34	34	0	100,00%
107	36	35	1	97,22%
108	30	29	1	96,67%
109	47	47	0	100,00%
111	35	35	0	100,00%
113	29	29	0	100,00%
114	27	27	0	100,00%
115	31	31	0	100,00%
117	25	25	0	100,00%
118	37	37	0	100,00%
119	32	32	0	100,00%
122	45	45	0	100,00%
123	24	24	0	100,00%
124	25	25	0	100,00%
200	44	44	0	100,00%
201	44	44	0	100,00%
202	26	26	0	100,00%
205	44	44	0	100,00%
207	29	29	0	100,00%
208	52	52	0	100,00%
209	46	46	0	100,00%
210	45	28	17	62,22%
212	45	45	0	100,00%
213	55	55	0	100,00%
214	38	38	0	100,00%
215	56	56	0	100,00%
217	36	36	0	100,00%
219	36	36	0	100,00%
220	36	36	0	100,00%
221	38	38	0	100,00%
222	38	38	0	100,00%

223	40	40	0	100,00%
228	38	19	19	50,00%
230	41	41	0	100,00%
231	31	31	0	100,00%
233	51	51	0	100,00%
234	46	46	0	100,00%

Table 4.2 Results of evaluation QRS detection using MIT/BIH database in the first 30s.

The following table shows the results obtained in the case in which we take only the first 5min of the records:

records	Totale beat	TP (Beats)	FP (Beats)	Positive Predictivity
100	371	371	0	100,00%
101	342	341	1	99,71%
102	366	366	0	100,00%
103	355	355	0	100,00%
105	417	417	0	100,00%
107	353	352	1	99,72%
109	433	341	91	78,94%
111	348	348	0	100,00%
113	289	289	0	100,00%
114	275	275	0	100,00%
115	316	316	0	100,00%
117	251	251	0	100,00%
118	362	362	0	100,00%
119	326	326	0	100,00%
122	422	422	0	100,00%
123	249	249	0	100,00%
124	252	252	0	100,00%
202	265	265	0	100,00%
205	455	455	0	100,00%
209	486	486	0	100,00%
212	463	463	0	100,00%
213	551	551	0	100,00%
214	383	269	108	71,35%
215	568	300	266	53,00%
217	363	363	0	100,00%
219	381	258	121	68,07%
220	354	354	0	100,00%

221	407	407	0	100,00%
222	367	367	0	100,00%
223	406	406	0	100,00%
230	397	397	0	100,00%
231	295	293	0	100,00%
233	518	518	0	100,00%
234	462	462	0	100,00%

Table 4.3 Results of evaluation QRS detection using MIT/BIH database

The following table shows results of the records which give the same number of beats as those of the MIT/BIH database detected by our implementation:

Records	Totale beat	TP (Beats)	FP (Beats)	FN (Beats)	(+p) Positive Predictivity
100	2273	2273	0	0	100%
102	2187	2187	0	0	100%
115	1953	1953	0	0	100%
117	1535	1535	0	0	100%
118	2278	2278	0	0	100%
121	1863	1863	0	0	100%
122	2476	2476	0	0	100%
209	3005	3005	0	0	100%
212	2748	2748	0	0	100%
220	2048	2048	0	0	100%
230	2256	2256	0	0	100%
231	1571	1571	0	0	100%

Table 4.4 Results of evaluation QRS detection using MIT/BIH database.

Conclusion

From the obtained results it's obvious that the used filters in the implemented algorithm as described by Pan and Tompkins paper [20], are well designed and have a good impact to reduce the noise present in the ECG signals. The authors proposed an adaptive thresholding method and some free parameter like MWI, which is fixed to 30 samples according to the width of the QRS complex which equal to 150 ms (because the sampling frequency of the signal equal to 360 Hz), to detect the QRS complexes. The results obtained by tuning empirically the MWI parameter proposed in our approach shows an improvement in term of accuracy compared with the results published in the original paper.

From the conducted experiments we conclude that the QRS complexes detection with our implementation based on the Pan and Tompkins paper it yields to better detection then the original algorithm for some ECG records, and this due in our opinion to many factors, for example, despite the complexity of the signal, the adaptive threshold, many free parameters like MWI fixed to 30 samples empirically in Pan and Tompkins paper. This is an important parameter for the good QRS complex detection process. Also from the experiments we showed that the MWI is an important parameter just by tuning this parameter to 54 samples instead of 30 samples published in the original paper. We were able to boost the results in term of QRS complex detection. Another important factor explored in our experimental phase is the delay between the true detection given by the MIT/BIH in the ATR file and our detection beats.

In addition to the tuning of the precedent parameters another round of experiment is proposed to explore the capability of the capability of the algorithm when it's sectioned with only a portion of (30s and 5 min) of the signal. From the obtained results concerning the first case we see that the algorithm was capable to detect all the beats with high accuracy (almost 100%). For the second case, even when sometimes gives a low accuracy for some records (e.g.:215...) it still behave well and yields to a high accuracy for the majority of the records.

Finally we can conclude that the our implementation in average works well, although for some records yields to low detection and this is owing to the adaptive threshold procedure.

Conclusion and Future work

In this work our sole objective was to implement the Pan and Tompkins algorithm for automatic QRS complex detection. As described by Pan and Tompkins in their published work this algorithm is based on slope, amplitude and width information. The algorithm contains two phases the pre-processing stage and the decision roles. In the pre-processing stage many filtering steps are used and a nonlinear transformation to square the signal at some point to emphasize the QRS complexes and reduce unwanted parts of the signal. For the decision stage a threshold is necessary to detect the QRS complexes. The threshold applied in the implemented algorithm of Pan and Tompkins is adaptive to the ECG signal because the signals don't have the same shape between people.

The results demonstrated that our implementation works well on the MIT/BIH database. Especially in detecting normal QRS complexes, but it has rather poor performance when it comes to detecting abnormal (e.g. wider) QRS complexes.

The implemented algorithm has a very high rate in term of detection for the QRS complex. However the weak point of the algorithm is the low rate in term of detection of the QRS complex in some records of the MIT/BIH database. The low detection rate can be justified, there are cases in which the amplitude of the P wave is similar to that of QRS complexes, or the morphology of the P wave is comparable with that of QRS complexes.

More investigation have to be given to the optimisation of the thresholds proposed in Pan and Tomkins paper: try to find a best method for estimate the adaptive threshold, for the instance using the metaheuristic algorithm.

For this reason we propose as a future works, to use the new state of the art method based the wavelet transformation (WT). Which showed superior results compared with the Pan and Tompkins algorithm. Feature extraction is yet another useful technique in ECG signal analysis not explained by us. But it is very essential for classification of arrthymia. Hence a future work will be dedicated to feature extraction and classification.

References

[1] Richard E. Klabunde, "Cardiovascular Physiology Concepts," *Second Edition*, *Published by Lippincott Williams & Wilkins, ISBN*, 2011.

[2] Carlos Casillas, Rtac Americas, Guadalajara and Mexico, "*Heart Rate Monitor and Electrocardiograph Fundamentals*, "pp.7-8, March 2010.

[3] El Hassan El Mimouni, Mohammed Karim," Novel Real-Time FPGA-Based QRS Detector Using Adaptive Threshold with the Previous Smallest Peak Of ECG Signal," *Journal of Theoretical and Applied Information Technology, Vol 50*, 10th April 2013.

[4] Tony Curran and Gill Sheppard, "*Anatomy and Physiology of the Heart*,"pp.8, October 2011.

[5] Elizabeth M. Cherry and Flavio H, "*Heart Structure, Function and Arrhythmias*," Fenton Department of Biomedical Sciences, College of Veterinary Medicine, Cornell University, Ithaca, NY.

[6] Williams PL, Warwick R, "*Gray's Anatomy*,"37th edition, pp. 1598, 1989.

[7] Richard E. Klabunde, "*Cardiovascular Physiology Concepts, Cardiac cycle*," http://www.cvphysiology.com /Heart%20Disease/HD002.htm , September 4, 2009.

[8] Guyton, A, "*Textbook of Medical Physiology*," J.E. 11th Edition, 2006.

[9] Health Sciences Library of the University of Utah, "http://library.med.utah.edu/kw/pharm/hyper_heart1.html , "August 28, 2009.

[10] A.D. Waller, "*A demonstration on man of electromotive changes accompanying the heart beat*," Physiol. 8, pp.229-234, 1887.

[11] S Barron, "*The development of the electrocardiograph*," London, Cambridge Instrument Co, 1952.

[12] T Lewis, "Electro-cardiography and its importance in the clinical examination of heart affections," *British Medical Journal*, p.1421-1423, January 22nd, 1912, p.1479-1482, June 29th, 1912, p.65-67, July 13th, 1912.

[13] Jaya Prakash Sahoo, " *Analysis of ECG signal for Detection cardiac Arrhythmias*, " Department of Electronics and Communication Engineering, National Institute Of Technology, Rourkel Orissa, INDIA 2011.

[14] TCHP Education Consortium,"*ECG Rhythm Interpretation Primer*,"2004-2007.

[15] Nursecom Educational Technologies, "*Six Second ECG Guidebook*,"2003.

[16] Zeenat M. Kazi and P. C. Bhaskar, "Baseline wander and power line interference noise removal in ECG using digital IIR filter," *Indian Streams Research Journal*, Volume 4, Issue 5, June 2014.

[17] MaheshS.Chavan, RA.Agarwala, M.D.Uplane, "Design and implementation of Digital FIR Filter on ECG Signal for removal of Power line Interference," Wseas *Transactions On Signal Processing*, Volume 4, pp. 1790-5052, April 2008.

[18] N.V. Thakor, J.G. Webster and W.J.Thompkins, "Estimation of QRS complex power spectra for design of a QRS filter, " *IEEE Trans. Biomed. Eng*., vol. 31, pp. 702–705, 1984.

[19] Y.C. Yeha, and W. J. Wang, "QRS complexes detection for ECG signals The Difference Operation Method (DOM), " *Computer methods and programs in biomedicine, vol. 9*, pp. 245–254, 2008.

[20] J. Pan, W. J. Tompkins, "A real time QRS detection algorithm," *IEEE Trans. Biomed. Eng., vol. 32*, pp. 230– 236, 1985.

[21] X. Afonso, W.J. Tompkins, T. Nguyen, S. Luo, "ECG beat detection using filter banks, " *IEEE Trans. Biomed. Eng., vol. 46*, pp. 230-236, 1999.

[22] D. Beniteza, P.A. Gaydeckia, A. Zaidib, and A.P. Fitzpatrick, "The use of the Hilbert transform in ECG signal analysis," *Computers in Biology and Medicine, vol. 31*, pp.399–406, 2001.

[23] Bert-Uwe köhler, Carsten Hennig ,Reinhold Orglmeister, "The Principals of Software QRS Detection, "*IEEE Engineering In Medicine And Biology*, January/February 2002.

[24] G.M. Friesen, T.C. Jannett, M.A. Jadallah, S.L. Yates, S.R. Quint, H.T. Nagle, "A comparison of the noise sensitivity of nine QRS detection algorithms, " *IEEE Trans. Biomed. Eng. Vol.37*, pp.85–98, 1990.

[25] Seema Nayak,Dr.M.K.Soni,Dr.Dipali Bansal, " Filtering Techniques For ECG Signal Processing, " *IJREAS Vol.2,Issue 2*,pp.2249-3905,February 2012.

[26] Zainab Mizwan et al, "Study and Review of the Biomedical Signals With Respect To Different Methodologies," *International Journal of Computer Science and Information Technologies, Vol. 5 (2)*, pp.1307-1309, 2014.

[27] Tim Starr, "*Filtering A Noisy ECG Signal Using Digital Techniques*," April 19, 2005.

[28] H.G. Goovaerts, H .H. Ros .T.J. Vanden Akker, and H. Schneider, " A digital QRS detector based on the principal of contour limiting," *IEEE Trans .Biomed .Eng, Vol.BEM-23*, P.54, 1976.

[29] N.V. Thakor , J. G .Webster , and W.J.Tompkins, " Optional QRS detector ," *Med. Biol .Eng. comput, vol.21*, pp.343-350,1983.

[30] P.A.Lynn, " online digital filter for biological signal: some fast designs for a small computer, " *Med .Biol .Eng. Comput ,Vol 15*,pp.535-540, 1997.

[31] Valtino X. Afonso, "*ECG QRS Detection," Biomedical digital signal processing*, "pp 236-264, 1993.

[32] J. Pan, W. J. Tompkins, ERRATA. *IEEE Trans, Biomed. Eng*. July 1985.

[33] Massachusetts institute of technology. MIT-BIH ECG database. Available, http://physionet.org/physiobank/database/mitdb/.

[34] Cem Sakarya ,"*R-Peak Detection With Wavelet Transform*," University Of Çukurova Institute Of Natural And Applied Sciences,pp.7-12, ADANA, 2013.

[35] Zainab Mizwan et al, " Study and Review of the Biomedical Signals With Respect To Different Methodologies*, "(IJCSIT) International Journal of Computer Science and Information Technologies*, Vol. 5, pp.1307-1309, 2014